UNIVERSITAT POLITÈCNICA DE CATALUNYA
BARCELONATECH
Escola Superior d'Enginyeries Industrial, Aeroespacial i Audiovisual de Terrassa

UNIVERSITAT POLITÈCNICA DE CATALUNYA

BACHELOR'S DEGREE IN AEROSPACE TECHONOLOGIES ENGINEERING

BACHELOR'S THESIS - REPORT

Computational studies of non-viscous and viscous fluid flows

Author:
PÉREZ RICARDO, Carlos

Director:
OLIVA LLENA, Assensi

Co-director:
PÉREZ SEGARRA, Carles-David

June 10^{th}, 2019

Abstract

This Bachelor's Degree Thesis consists on a computational study of non-viscous and viscous fluid flows interacting with different external conditions and solid objects.

The governing equations of fluid dynamics are Navier-Stokes equations. NS equations are differentiate partial equations that are transformed into numerical expressions that can be computed.

Simulations with the computer are runned for different reference cases for which a previous solution has been obtained analytically or by researchers, beforehand.

The principles, solvers and methods used to achieve a solution for the simulations can be extrapolated to more complex problems.

Acknowledgements

I would like to thank to the people who has been involved in this project and who has helped me during its development.

Firstly, I would like to express my gratitude to the Universitat Politècnica Catalunya, especially to l'Escola Tècnica Superior d'Enginyeries Industrial, Aeronàutica i Audiovisuals de Terrassa. These four years have been a tough process but the education received and preparation have been extraordinary.

Secondly, I would like to thank to the director of my project, Dr. Asenssi Oliva Llena, for the supervision and guidance of the work.

I would like to thank also to the CTTC (Centre Tecnològic de Transferència de Calor), especially to the collaboration of Dr. Carles-David Pérez Segarra, who has been involved during all the project and has been a great help with his supervision and knowledge about the subject; and to Dr. Francesc Xavier Trias Miquel aroused a curiosity about the power of Computational Fluid Dynamics (CFD).

Finally, I would like to thank to my professors during these four years of Bachelor's Degree and to my classmates who have accompanied me and have given their support and advice during this process.

Contents

List of Figures

List of Tables

Glossary

Symbol	Description	Units
t	Time	[s]
x	Coordinate	[m]
y	Coordinate	[m]
Ψ	Stream function	[-]
ϕ	Potential function	[-]
f	Face indicator	[-]
$\dot{m}$	Mass flux	[kg/m^2]
c	Chord of the airfoil	[m]
α	Angle of attack	[rad]
t	time	[s]
ρ	Density	$[kg/m^3]$
μ	Dynamic viscosity	[Pa $\cdot$ s]
ν	Kinematic viscosity	$[m^2/s]$
k	Thermal conductivity	[W/(m·K)]
c_p	Specific heat	[J/kg·K]
M	Mach number	[-]
a	Speed of sound	[m/s]
V	Module of velocity	[m/s]
u	Velocity in the x-direction	[m/s]
v	Velocity in the y-direction	[m/s]
p	Pressure	[Pa]
Re	Reynolds number	[-]
Pe	Péclet number	[-]
Γ	Diffusion coefficient	[-]
CV	Control Volume	[-]
FSM	Fractional Step Method	[-]
FVM	Finite Volume Method	[-]
HH theorem	Helmholtz-Hodge theorem	[-]
CFD	Computational Fluid Dynamics	[-]
BOM	Blocking Off Method	[-]
GS	Gauss-Seidel solver	[-]
TDMA	Tridiagonal Matrix Algorithm	[-]

Table 0.1: Glossary of terms

1 Introduction

1.1 Aim

Study for the computational resolution of conservation equations of mass, momentum and energy in fluid-body problems. The main goal of the project is to determine the changes occurred in a fluid when contacting with a solid body using different methods, assumptions, schemes and solvers.

1.2 Scope

The main objectives to achieve are:

- Study of the potential flow in a channel of constant section and around a solid object such as a cylinder or a NACA airfoil.
- Study of the variation in temperature, pressure, velocity and density in a parallel flux in a channel or around a cylinder.
- Solving the system of equations using different solver methods: Gauss-Seidel, line-by-line, TDMA...
- Solving Navier-Stokes equations using different methods: implicit, explicit, Crank-Nicholson...
- Study of the Conduction-Diffusion equation for different problems in which the velocity field is known.
- Study of a turbulence case using FSM.
- Comparison when possible between the results obtained using the developed software and the results obtained by analytic means or by previous researches.
- Drafting of the report in which there will be a theoretical explanation of the equations, and the results obtained.
- Programming the solving codes in language C++ using the platform *Visual Studio Code*. For the plots and graphs, *MATLAB*® will be used.
- Study of the computational costs of the codes developed during the realisation of the project and environmental impact.

1.3 Requirements

The requirements of the Bachelor's Thesis are the following:

- The Project dedication limit is 300 hours (12 ECTS).
- All academic documents will be written in English.
- The deadline of the Project is June 10th, 2019.
- The presentation of the Project will be held between July 8th and July 19th.
- All the programs have to be developed in language C++ without using any kind of simplifying solvers or software developed by another user.
- For plotting graphs (heat maps, vector fields, y-x graphs, isotherms, streamlines...) MATLAB® will be used. MATLAB® will be only used to represent the data obtained in a graph, other post-process program could be used.

1.4 State of the art and justification

The main justification of this study is to learn and understand the physics, assumptions made and methods used to solve problems in which a fluid is interacting with a solid body and to understand the heat and mass transfer and fluid mechanics behind.

The governing equations are Navier-Stokes equations. NS equations are partial differentiate equations that describe the dynamics of the fluid. They are composed of: continuity equation or mass conservation (Eq.1.1), conservation of momentum (Eq.1.2) and energy conservation (Eq.1.3).

$$\frac{\partial \rho}{\partial t} + \nabla \cdot (\rho \vec{v}) = 0 \tag{1.1}$$

$$\rho(\frac{\partial \vec{v}}{\partial t} + \vec{v} \cdot \nabla \vec{v}) = -\nabla p + \nabla \cdot \bar{\bar{\tau}} + \rho \vec{g} \tag{1.2}$$

$$\rho c_v(\frac{\partial T}{\partial t} + \vec{v} \cdot \nabla T) = \nabla \cdot (\lambda \nabla T) - \nabla \cdot \vec{q}^R - p \nabla \cdot \vec{v} + \vec{\tau} : \nabla \vec{v} \tag{1.3}$$

The solution of momentum equation is a velocity field that satisfy all equations (x, y, z) in each point of the domain and in each instant of time.

Due to the non-linearity of the convective term, and the coupling between the equations, they are unable to solve analytically. Therefore, they are solved numerically with different methods and solvers.

Furthermore, the non-linearity and unpredictability of physical phenomena that describe them make the research and development in this area limited. Particularly, turbulence is one of the most unpredictable of all physical phenomena that up to now it has not been solved. Turbulence can be defined as any pattern of fluid motion characterised by chaotic changes in pressure and flow velocity.

The resolution of these equations are of great interest among engineering and science. Under some hypotheses and after the great effort made by many engineers and scientists years before, a solution of the problem can be obtained for some cases. However, sometimes to obtain the solution a high computational cost and time is needed.

Nowadays, with the huge evolution in computers occurred in the last 10 years, especially in the CPU (Central Processing Unit) and in the RAM memories (Random Access Memory), has increased the speed and potential of calculus that years before where hardly impossible to imagine.

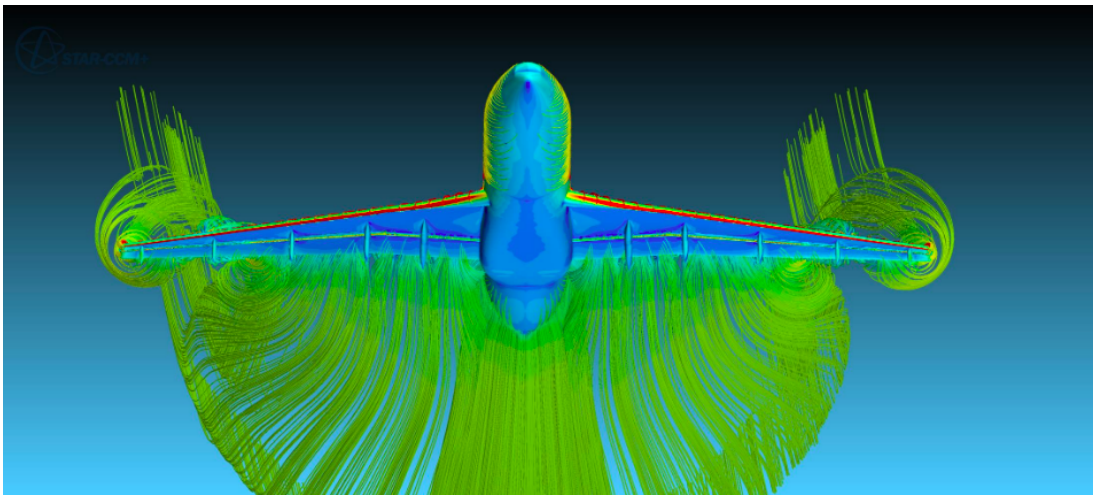

Figure 1.1: Numerical simulation of DLR-F11 high lift configuration using STAR CCM+ (extracted from [1])

Several programs and software able to solve Navier-Stokes equations and turbulence have appeared recently. Some of them are open source programs (*OpenFoam*) while others are mainly commercial: *Autodesk CFD*, *Fluent* in Ansys, *Star CCM+* from Siemens or the Toolbox *CFDTool* in MATLAB.

Figure 1.2: Most used CFD software

These software is used by companies, at University or even at user level is capable of solving the interaction between a fluid with a solid, and to determine the value

of parameters like temperature, velocity, pressure, density, heat, energy... These software are given the name of CFD (Computational Fluid Dynamics).

Most of the software mentioned before uses turbulence resolution methods. The most popular ones are:

- DNS (Direct Numerical Solution)
- RANS (Reynolds Average Numerical Solution)
- LES (Large eddy simulation)

Simulations offer estimations and allow people to analyse big complex problems for which there is no analytic solution yet. Once a model is determined, inserting the code with the actions in the computer, results can be achieved.

Nevertheless, the main inconvenience is that sometimes the most suitable way to solve a given equation leads to a huge amount of computational time and money that the user cannot afford. Although, with new technologies arrivals and developments these aspects will be diminished in the years yet to come.

The idea of the Project is to explain and understand the main ideas of the physical, thermodynamic, aerodynamic principles used by this software and being able to solve some fluid-body problems.

1.5 Motivation

During these four years of Bachelor's Degree, an passion has grown up about CFD. One of my main interests is to understand and being able to compute the behaviour of a fluid in motion interacting with different external conditions and solid objects.

Subjects such as *Aerodynamics*, *Heat and mass transfer*, *Aircraft's design* or *Analysis of Thermal and Fluid dynamics issues in industrial and/or aeronautical systems and equipment* have increased my curiosity in this matter.

With computer science, it is opening a powerful tool that can provide us the means to solve complex physical problems.

2 Introduction to numerical analysis

In this chapter, there will be explained what numerical analysis consists. An explanation of several mathematical principles will be explained briefly with the purpose of converting the physical problem into a numerical problem. The method used would be Finite Volume Method.

"The Finite Volume Method (FVM) is a numerical technique that transforms the partial differential equations representing conservation laws over differential volumes into discrete algebraic equations over finite volumes (or elements or cells)." [2]

Finite Volume Method (FVM) enables to solve numerically Navier-Stokes equations (Eq.1.1, Eq.1.2 and Eq.1.3). The first step is to discretize the geometric domain then the partial differential equations are discretized/transformed into algebraic equations by integrating them over each discrete element.

2.1 Mathematical theorems and operators

During the elaboration of this project there will be needed the value in a node in which is totally unknown, particularly important when first-derivative or second-derivative appear. Taylor series expansion will be commonly used to obtain the desired value.

$$\phi_i = \phi_i$$

$$\phi_{i+1} = \phi_i + h_{i+1}\partial_x\phi_i + \frac{h_{i+1}^2}{2!}\partial_{xx}\phi_i + \frac{h_{i+1}^3}{3!}\partial_{xxx}\phi_i + ...$$

$$\phi_{i-1} = \phi_i - h_{i-1}\partial_x\phi_i + \frac{h_{i-1}^2}{2!}\partial_{xx}\phi_i - \frac{h_{i-1}^3}{3!}\partial_{xxx}\phi_i + ...$$

Taylor series expansion will also allow to calculate the local truncation error of using a particular scheme.

On the other hand, terms like partial derivatives, divergence or scalar product would be mentioned in Navier-Stokes equations in order to convert them into numerically expressions. Generally, transient or unsteady terms will be converted as:

$$\frac{\partial\phi}{\partial t} = \frac{\phi_{new} - \phi_{previous}}{\Delta t} \tag{2.1}$$

For scalar products, typically for calculation of mass fluxes, will be computed taking into account the direction $\vec{n}$ at the faces of the CV, where $\vec{n}$ is the normal vector at face plane pointing out.

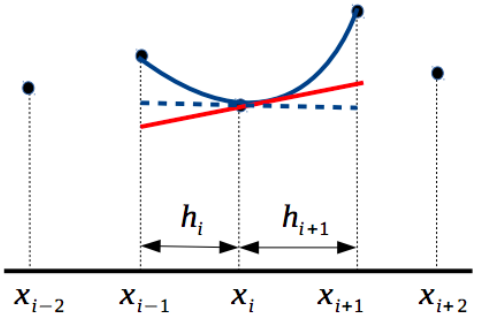

Figure 2.1: FVM discretization (extracted from [3])

Furthermore, divergence theorem, also known as Gauss's theorem or Ostrogradsky's theorem, will be also used to transform triple integrals into a second integral with a scalar product.

$$\iiint_V (\nabla \cdot \vec{F}) = \oint_S (\vec{F} \cdot \vec{n}) dS \tag{2.2}$$

Divergence theorem simplifies the integral into adequate terms to integrate numerically.

2.2 System of equations' solvers

After converting NS equations into numerical expressions, a system of equations will have to be solved using different solvers. In this project two main solvers will be used: Gauss Seidel and TDMA.

2.2.0.1 Gauss-Seidel

Gauss-Seidel is an iterative method used to solve a linear system of equations. GS is a point-by-point solver. For the case *Parallel flow in a duct* (explained later in chapter *3. Potential Flow*) the equation to solve has the following structure [4].

$$a_p \cdot \phi_p = a_e \cdot \phi_e + a_w \cdot \phi_w + a_n \cdot \phi_n + a_s \cdot \phi_s + b_p$$

Therefore, for the calculation of ϕ at the node P (ϕ_p):

$$\phi_p = \frac{a_e \cdot \phi_e + a_w \cdot \phi_w + a_n \cdot \phi_n + a_s \cdot \phi_s + b_p}{a_p}$$

The value of ϕ in the domain is calculated in every point, taking into account the values of the nodes nearby.

2.2.0.2 TMDA : Line-by-line

Line-by-line method is a TDMA solver (Tri-Diagonal Matrix Algorithm) which is only valid for matrix where its main, upper and lower diagonals are different from zero, the rest of terms are null or can be considered as almost zero (if the matrix is diagonal dominant).

$$A = \begin{pmatrix} a_{p_1} & a_{e_1} & 0 & 0 & 0 & \cdots & 0 \\ a_{w_2} & a_{p_2} & a_{e_2} & 0 & 0 & \cdots & 0 \\ 0 & a_{w_3} & a_{p_3} & a_{e_3} & 0 & \cdots & 0 \\ \vdots & \vdots & \vdots & \ddots & \vdots & \vdots & \vdots \\ 0 & \cdots & 0 & a_{w_{n-2}} & a_{p_{n-2}} & a_{e_{n-2}} & 0 \\ 0 & \cdots & 0 & 0 & a_{w_{n-1}} & a_{p_{n-1}} & a_{e_{n-1}} \\ 0 & \cdots & 0 & 0 & 0 & a_{w_n} & a_{p_n} \end{pmatrix}$$

TDMA solver is capable of solving the N equations (N : number of rows of matrix A) which have the following structure:

$$a_p \cdot \phi_p = a_e \cdot \phi_e + a_w \cdot \phi_w + b_p$$

However, for 2D cases it is possible to transform the equation into (line-by-line method):

$$a_p \cdot \phi_p = a_e \cdot \phi_e + a_w \cdot \phi_w + b_p^*$$

where: $b_p^* = a_n \cdot \phi_n + a_s \cdot \phi_s + b_p$

TDMA method is quicker than Gauss-Seidel method. For several cases TDMA does not need a convergence criterion, so it is a direct method, whereas Gauss-Seidel method is an iterative method so a loop is needed to achieve the convergence.

However, TDMA cannot be used for every case, only when the matrix is tri-diagonal or and assumption can be made if the matrix is diagonal dominant.

3 Potential Flow

In this chapter, there will be developed the potential flow (Ψ) solution in a duct of constant section, around a cylinder and a NACA airfoil. The potential flow solution denote the streamlines of the flow around solid objects.

3.1 Introduction

Potential flow describes the velocity field as the gradient of a scalar function: the velocity potential. In the case of an incompressible flow the velocity potential satisfies Laplace's equation, and potential theory is applicable. [5]

The flow region around aerodynamic bodies can be divided into:

- **Boundary Layer region**. Area closed to the walls of the body with a small thickness. High gradient of pressure and temperature are produced within, due to the friction, heat transfer and mainly turbulence.
- **Inviscid region**. Rest of the domain in which the effects of friction and heat losses can be neglected.

The Inviscid region is governed by Euler's equations:

$$\frac{\partial \rho}{\partial t} + \nabla \cdot (\rho \vec{v}) = 0 \qquad (Conservation\ of\ Mass) \tag{3.1}$$

$$\frac{\partial (\rho \vec{v})}{\partial t} + \nabla \cdot (\rho \vec{v} \vec{v}) = -\nabla p \qquad (Conservation\ of\ Momentum) \tag{3.2}$$

$$\frac{\partial E}{\partial t} + \nabla \cdot (E \vec{v}) = -\nabla \cdot (p \vec{v}) \qquad (Conservation\ of\ Energy) \tag{3.3}$$

where E represents the total energy (kinetic + internal) per unit of volume.

The external flows around bodies can be considered as inviscid (frictionless) and irrotational (the fluid particles are not rotating). Therefore, the viscous effects are limited to a thin layer next to the body called the boundary layer [5].

A solution of the external flow can be obtained: potential flow.

3.2 Potential function

A potential function ϕ(x,y,t) can be defined as a continuous function that satisfies the conservation of mass and momentum, assuming incompressible, inviscid and irrotational flow.

For a scalar function ϕ, Eq.3.4 is satisfied, furthermore by definition, the irrotational flow follows Eq.3.5:

$$\nabla \times \nabla\phi = 0 \qquad (3.4) \qquad\qquad \nabla \times \vec{v} = 0 \qquad (3.5)$$

Therefore, a velocity potential function ϕ(x,y,z,t) can be obtained as:

$$\vec{v} = \nabla\phi \tag{3.6}$$

The components of velocity in Cartesian coordinates are:

$$u = \frac{d\phi}{dx} \qquad\qquad v = \frac{d\phi}{dy} \qquad\qquad w = \frac{d\phi}{dz}$$

The velocity field must satisfy the conservation of mass equation. Replacing each term, and introducing the definition of each velocity component:

$$\rho(\frac{\partial u}{dx} + \frac{\partial v}{dy} + \frac{\partial w}{dz}) = 0 \;\rightarrow\; \frac{\partial^2(\phi)}{dx^2} + \frac{\partial^2(\phi)}{dy^2} + \frac{\partial^2(\phi)}{dz^2} = 0 \tag{3.7}$$

A Laplace equation is obtained:

$$\nabla^2\phi = 0 \tag{3.8}$$

The Laplace equation can be solved in different coordinate systems: cartesian, cylindrical or spherical (see more in [5]).

Lines of constant ϕ are called *potential lines*. In two dimensions, the expression of ϕ is (Eq.3.9):

$$d\phi = \frac{\partial(\phi)}{\partial x}dx + \frac{\partial(\phi)}{\partial y}dy \;\rightarrow\; d\phi = udx + vdy \tag{3.9}$$

Since d$\phi = 0$ along a potential line, the final expression is:

$$\frac{dy}{dx} = -\frac{u}{v} \tag{3.10}$$

Recall that streamlines are lines tangent to the velocity; $\frac{dy}{dx} = -\frac{u}{v}$. Streamlines are perpendicular to the potential lines and a new scalar function defining the streamlines can be described, named as Stream Function Ψ. The relations between potential and stream functions are:

$$u = \frac{\partial\phi}{\partial x} = \frac{\partial\Psi}{\partial y} \quad (3.11) \qquad v = \frac{\partial\phi}{\partial y} = -\frac{\partial\Psi}{\partial x} \quad (3.12)$$

These equations are also known as the Cauchy-Riemann equations.

3.3 Stream function

For a 2D potential flow, assuming inviscid and irrotational flow a stream function can be determined [6]. The velocities expressed as a function of the stream function are:

$$v_x = \frac{\rho_0}{\rho}\frac{d\Psi}{dY} \qquad (3.13) \qquad v_y = -\frac{\rho_0}{\rho}\frac{d\Psi}{dX} \qquad (3.14)$$

where ρ_0 is the reference density for determined conditions (p_o, T_0).

Obviously, the stream function verifies the conservation of mass or continuity equation ($\nabla \cdot (p\vec{v} = 0)$. Besides that, vorticity $\vec{\omega}$ is defined as:

$$\vec{\omega} = \nabla x \vec{v} \qquad (3.15)$$

Substituting, it is obtained:

$$\frac{\partial}{\partial x}(\frac{\rho_0}{\rho}\frac{d\Psi}{dx}) + \frac{\partial}{\partial y}(\frac{\rho_0}{\rho}\frac{d\Psi}{dy}) = -\omega_z \qquad (3.16)$$

Given that the flow is considered irrotational ($\omega_z = 0$).

$$\frac{\partial}{\partial x}(\frac{\rho_0}{\rho}\frac{d\Psi}{dx}) + \frac{\partial}{\partial y}(\frac{\rho_0}{\rho}\frac{d\Psi}{dy}) = 0$$

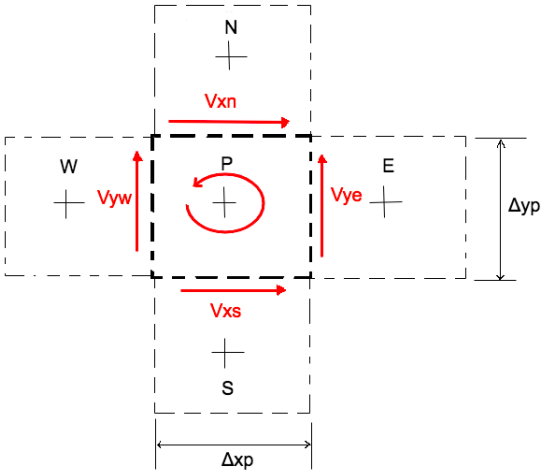

Figure 3.1: Circulation in an intern CV

The circulation in an intern Control Volume (CV), such as the one in Figure 3.1 is:

$$\Gamma = v_{ye} \triangle y_P - v_{xn} \triangle x_p - v_{yw} \triangle y_p + v_{xs} \triangle x_p = 0 \qquad (3.17)$$

The velocities at the faces of the Control Volume (CV) are obtained using Taylor series expansions (explained in section *2. Introduction to numerical analysis*):

$$V_{ye} = -\frac{\rho_0}{\rho_e}\frac{d\Psi}{dx}\Big|_e \approx \frac{-\rho_0}{\rho_e}\frac{\Psi_E - \Psi_P}{d_{PE}} \qquad V_{yw} = \frac{\rho_0}{\rho_w}\frac{d\Psi}{dx}\Big|_w \approx \frac{\rho_0}{\rho_w}\frac{\Psi_W - \Psi_P}{d_{PW}}$$

$$V_{xn} = \frac{\rho_0}{\rho_n}\frac{d\Psi}{dy}\Big|_n \approx \frac{\rho_0}{\rho_n}\frac{\Psi_N - \Psi_P}{d_{PN}} \qquad V_{xs} = -\frac{\rho_0}{\rho_s}\frac{d\Psi}{dy}\Big|_s \approx \frac{-\rho_0}{\rho_s}\frac{\Psi_S - \Psi_P}{d_{PS}}$$

Introducing the definition of velocities in the Eq. 3.17.

$$-\frac{\rho_0}{\rho_e}\frac{\Psi_E - \Psi_P}{d_{PE}} \triangle y_p - \frac{\rho_0}{\rho_n}\frac{\Psi_N - \Psi_P}{d_{PN}} \triangle x_p + \frac{\rho_0}{\rho_w}\frac{\Psi_P - \Psi_W}{d_{PW}} \triangle y_p + \frac{\rho_0}{\rho_s}\frac{\Psi_P - \Psi_S}{d_{PS}} \triangle y_s = 0$$

Finally, the equation of discretization (Eq.3.18) can be resumed in:

$$a_P\Psi_P = a_E\Psi_E + a_W\Psi_W + a_N\Psi_N + a_S\Psi_S + b_P \tag{3.18}$$

where each term corresponds to:

$$a_E = \frac{\rho_0}{\rho_e}\frac{\triangle y_p}{d_{PE}}\ ; \qquad a_W = \frac{\rho_0}{\rho_W}\frac{\triangle y_p}{d_{PW}}\ ; \qquad a_N = \frac{\rho_0}{\rho_N}\frac{\triangle y_p}{d_{PN}}\ ;$$

$$a_S = \frac{\rho_0}{\rho_S}\frac{\triangle y_p}{d_{PS}}\ ; \qquad a_P = a_E + a_W + a_N + a_S\ ; \qquad b_P = 0$$

3.4 Potential flow problems

In this section, different potential flow cases will be solved considering that the flow is incompressible (ρ is considered constant). The solution obtained will correspond to the streamlines of the flow.

Streamlines are a family of curves that are instantaneously tangent to the velocity vector of the flow. These show the direction in which a massless fluid element will travel at any point in time [7]. If the flow is steady, streamlines will be equal to pathlines. Pathlines describe the path of a particle in a flow.

3.4.1 Parallel flow in a duct

A constant and parallel flow ($u_x = u$, $v_y = 0$) is moving towards a duct of constant section. Integrating Eq. 3.13 and Eq. 3.14 along X and Y, the stream function Ψ has the following expression (Eq. 3.19):

$$\Psi = \frac{\rho_0}{\rho} u_x \cdot Y + \frac{\rho_0}{\rho} v_y \cdot X + k \tag{3.19}$$

In this case, the velocity in y-direction is null and the value of the constant k is imposed as 0. The following equation (Eq.3.20) is obtained :

$$\Psi = \frac{\rho_0}{\rho} u_x \cdot Y \tag{3.20}$$

The analytic solution correspond to lines parallel to the x-axis, that increase their value has Y increases.

A program to solve the problem has been developed *PF-ParallelFlow.cpp* (Code in *Annex I*). With *MATLAB*®, the streamlines of the solution have been represented in Figure 3.2. As expected the solution corresponds to parallel lines along the x-axis. Besides that, potential lines ϕ would be parallel lines along the y-axis perpendicular to the streamlines.

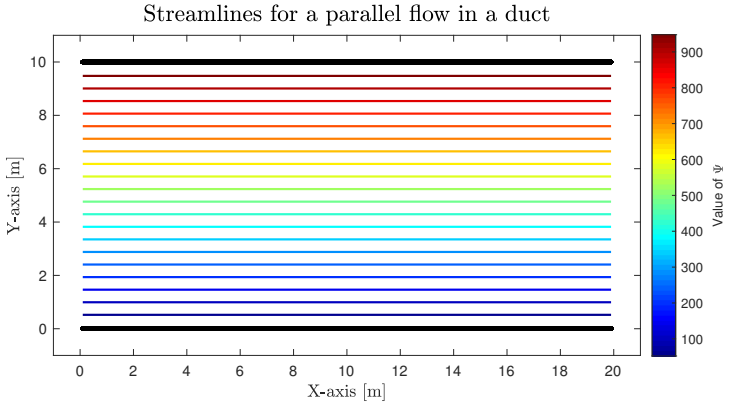

Figure 3.2: Streamlines of a parallel flow in a duct

The walls are considered as streamlines, moreover by considering potential flow there is no friction, therefore the velocity at the walls is constant and there is no consideration of a boundary layer.

In this case, for the solver two different solvers have been implemented: Gauss-Seidel and TDMA line-by-line. These solvers are explained in chapter *2. Introduction to numerical analysis.*

3.4.2 Flow around a cylinder

In this case, the mesh has to be determined carefully, a part of the mesh would be considered as solid and the other, part of fluid. *Blocking Off* method has been implemented to distinguish between the nodes of fluid and the ones of solid.

Blocking Off method evaluates if the centroid of the Control Volume (CV) is either in the fluid domain or in the solid domain. The higher dense the mesh is, the more accurate the discretization will be.

In Figure 3.3, the mesh of a cylinder in the middle of a duct has a dimension of 20x20 (Nx x Ny, where Nx and Ny are the number of divisions along the x-axis and y-axis); it is easy to observe that the shape of the cylinder is not well defined. Whereas in Figure 3.4, for the mesh of size 50x50, the definition has improved.

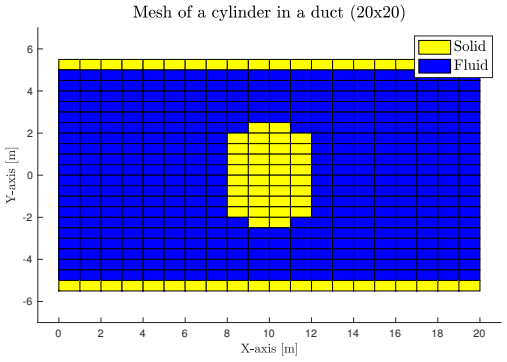

Figure 3.3: BOM - Cylinder with a mesh of dimensions 20x20

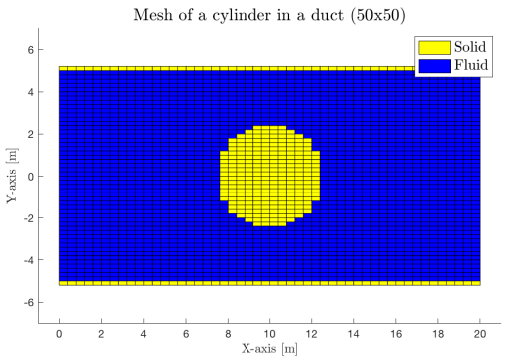

Figure 3.4: BOM - Cylinder with a mesh of dimensions 50x50

In this case, the dimensions of the problem are:

- Lenght of the duct : L = 20 m
- Height of the duct : H = 10 m
- Radius of the cylinder : R = 2.5 m
- $u_x = u_{inf} = 50\frac{m}{s}$
- $v_x = 0$

The Mach number for the entrance velocity is $M = \frac{v}{a} = \frac{50m/s}{340m/s} = 0.147$. Therefore, the flow can be considered incompressible (M<0.2).

The cylinder is centered in the middle of the channel. A program to solve the problem has been developed *PF-CylinderFlow.cpp* (Code in *Annex I*). In Figure 3.5, the solution of the streamlines around a cylinder can be observed.

The boundary of the cylinder is a streamline its self. When the flow is through the wall and the cylinder streamlines close their distance. In this case, terms such as friction, drag or turbulence are neglected when potential flow hypotheses are established.

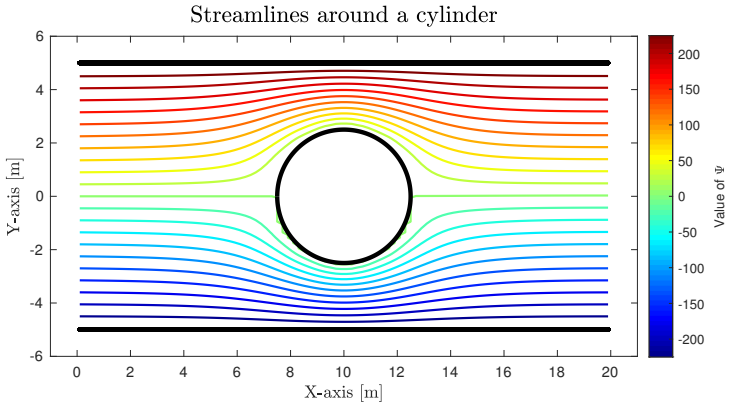

Figure 3.5: Streamlines around a cylinder

The boundary conditions established were the following:

- The velocity in the entrance has a constant value ($u_x = u_{inf}$ and $v_x = 0$). Therefore, stream function Ψ at the entrance is also known, substituting in the Eq.3.19.
- The stream function Ψ at the walls is known ($u_x = u_{inf}$ and $v_x = 0$). There is no normal velocity in the nodes in the wall, only tangential velocities.
- The shape of the cylinder corresponds to a stream line its self and it is a constant value.

An analytic solution to the flow around a cylinder (Eq. 3.21) can be obtained [8]. The solution is the superposition of the stream function of a uniform flux and a dipole.

$$\Psi = \Psi_U + \Psi_D = V_\infty r sen(\theta)(1 - \frac{R^2}{r^2}) \tag{3.21}$$

The next step would be to compare the obtained solution with the analytic. Because of the effect of the walls and their boundary conditions, there is a considerable difference between them, due to the fact that analytic solution does not take the walls into account.

In order to compare the solution obtained with the analytic solution correctly, there are two possibilities:

- Increase the distance between the cylinder and the walls of the channel, in order to reduce the interference.
- Establish new boundary conditions. The new boundary conditions will correspond to the analytic stream function obtained at the points of the wall.

In the first possibility, the maximum error obtained in a point is 3.15%. In Figure 3.6 and Figure 3.7 the analytic and the solution obtained with the program can be observed.

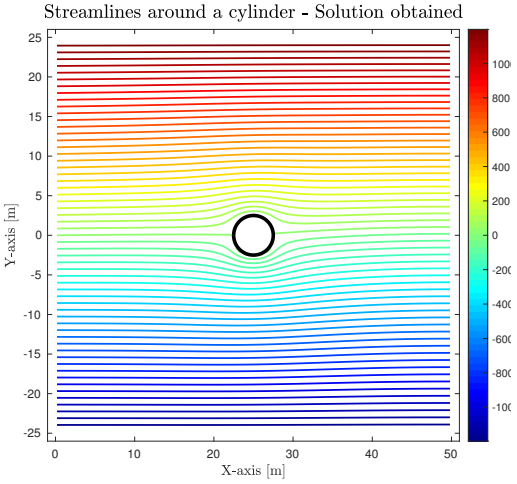

Figure 3.6: Stream Function Solution obtained with the solver - Case 1

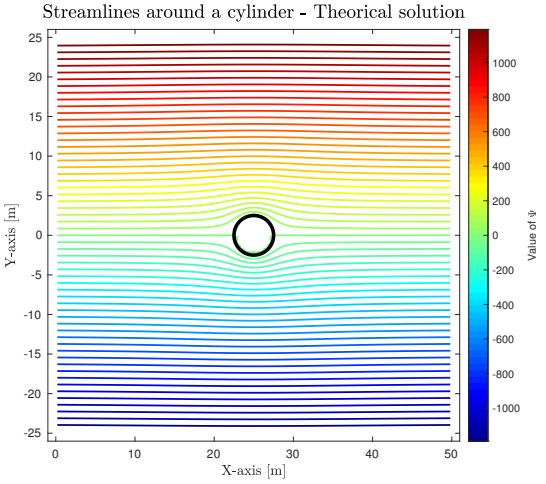

Figure 3.7: Analytical stream function solution - Case 1

While, for the second possibility the maximum error obtained in a point is 0%. Hence, it can be established that the program solves potential flow problem correctly. In Figure 3.8 and Figure 3.9, both solutions can be observed.

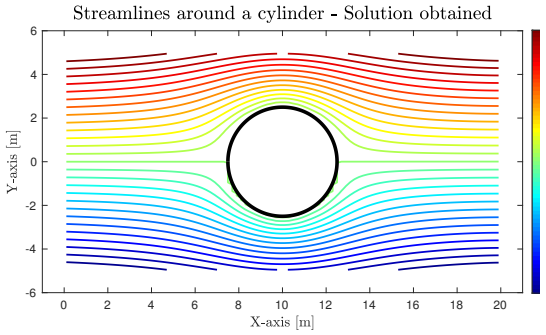

Figure 3.8: Stream Function Solution obtained with the solver - Case 2

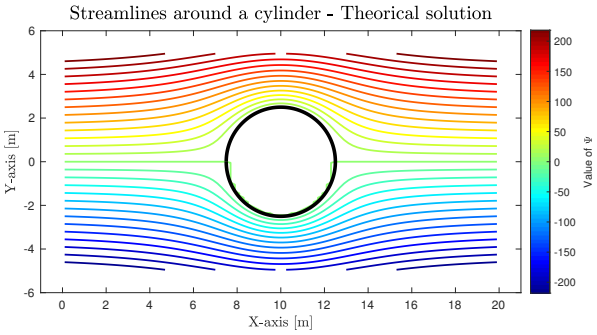

Figure 3.9: Analytical stream function solution - Case 2

3.4.3 Flow around a NACA airfoil

As done with the cylinder, BOM is used to determine the mesh and its boundary conditions. In this case a NACA airfoil is placed in the middle of a duct, meshes of dimensions 30x30 and 75x75 can be observed in Figure 3.10 and Figure 3.11, respectively:

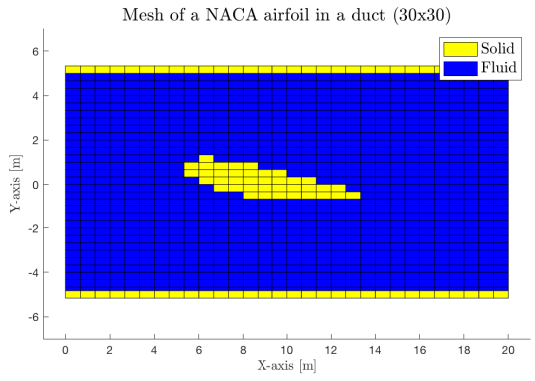

Figure 3.10: BOM - NACA profile with a mesh of dimensions 30x30

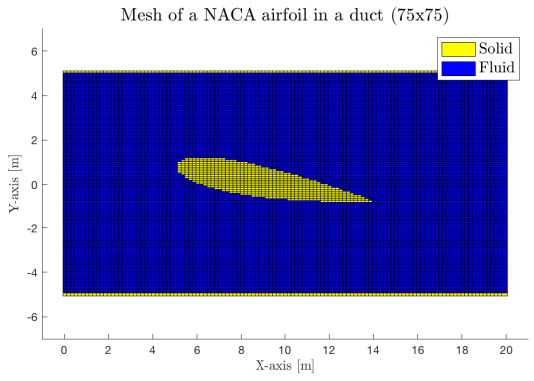

Figure 3.11: BOM - NACA profile with a mesh of dimensions 75x75

The dimensions of the problem are:

- Length of the duct : L = 20 m
- Height of the duct : H = 10 m

For the characteristics of the airfoil:

- Chord : c = 9 m
- Thickness : t = 1.5 m
- Angle of attack : $\alpha = 10^o$

And the velocity field (incompressible case) at the entrance is known:

- $u_x = u_{inf} = 50\frac{m}{s}$
- $v_x = 0$

A program to solve the problem has been developed in *PF-NACAFlow.cpp* (Code in *Annex I*). In Figure 3.12, the streamlines around a NACA airfoil can be observed. In this case the solution has been obtained under the hypotheses of potential flow and incompressible, therefore the flow around the NACA airfoil is attached, as it is for the cylinder solved in the previous sections.

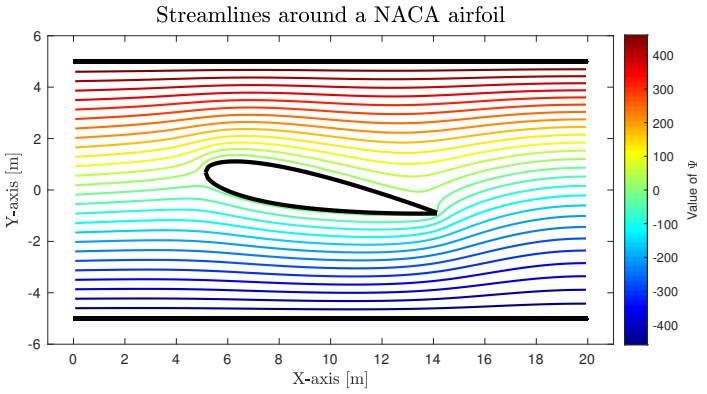

Figure 3.12: Streamlines around a NACA airfoil

As for the cylinder case, the boundary of the airfoil is a streamline its self, no friction is considered between the flow and the walls of the solid.

3.5 Potential flow resolution

In order to solve Potential flow problems the sequence of actions and calculations are resumed in Figure 3.13.

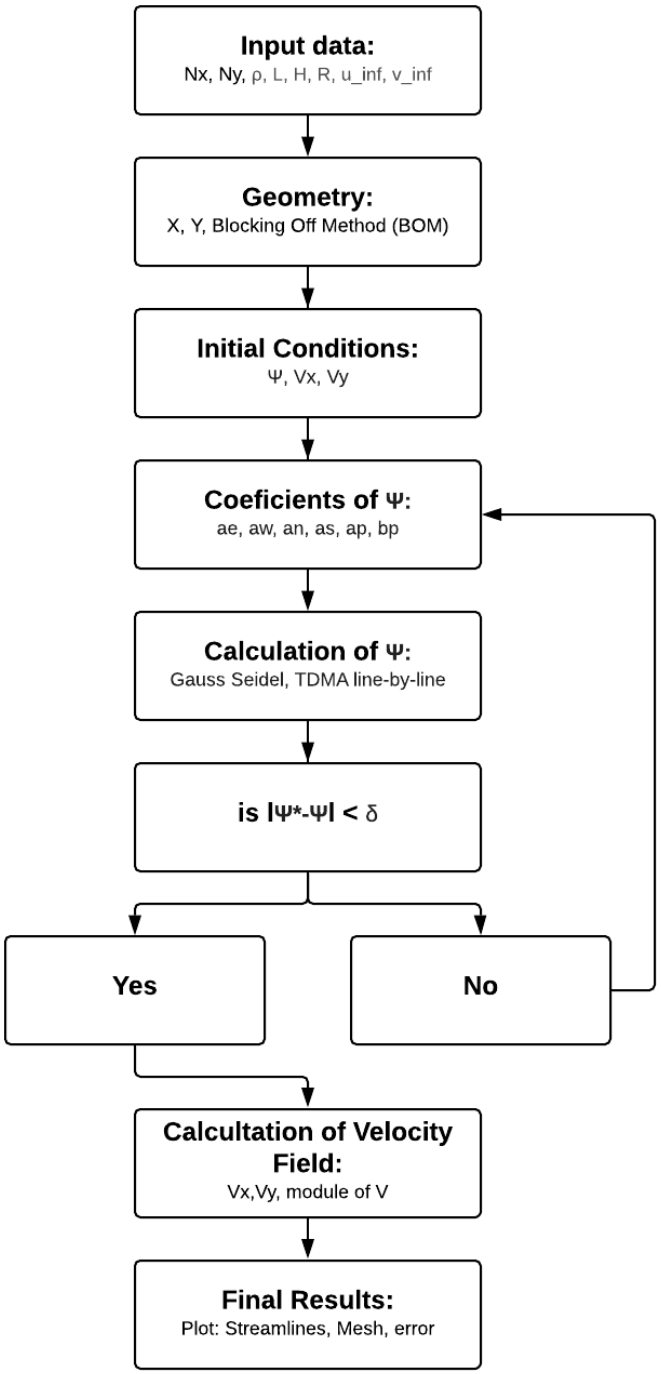

Figure 3.13: Diagram of the resolution of Potential Flow problem

3.6 Summary

During this chapter, the solution for a inviscid (frictionless), irrotational (the fluid particles are not rotating) and incompressible (densisty ρ considered constant in all the domain) flow around different objects in two dimensions has been developed.

As seen in Figure 3.2, in Figure 3.5 and in Figure 3.12 the obtained solutions have gone as expected in every case. Stremlines are not crossing and they are adapting to the geometry of the problem.

For the cases of the cylinder, NACA airfoil and the walls of the duct, the boundary of the object is considered a streamline its self, therefore the flow is considered completely attached which is not completely true.

For the case of the NACA airfoil, this assumption is fatal especially for high angles of attack or high thickness of the airfoil, where the flow could become turbulent and completely disattach from the surface.

During this chapter, it has been implemented two different methods to solve the system of equations: Gauss-Seidel and TDMA. Gauss-Seidel is a point-by-point solver and TDMA, which is only valid for matrices with a particularity.

4 Convection-diffusion

In this chapter, there will be developed the solution of the Convection-diffusion equation for several reference cases for which the velocity field is known.

4.1 Introduction

Convection is a physical process inside a fluid where a property is transported by the ordered motion of the flow. On the other hand, diffusion is a physical process physical process that occurs in a flow of gas in which some property is transported by the random motion of the molecules of the gas [9].

In the following sections, some new terms will be introduced to provide a ratio of the balance the of each physical term, which will define how the flow will tend to behave.

Another important aspect to solve in this section is the non-linearity of the convection term. To solve that fact, different schemes will be tested to obtain the desired solution.

4.2 Convection-diffusion equation

Navier-Stokes equations for perfect gases (c_v = constant) can be written as:

$$\underbrace{\frac{\partial \rho}{\partial t}}_{unsteady\ term} + \underbrace{\nabla \cdot (\rho \vec{v})}_{convective\ term} = 0 \tag{4.1}$$

$$\underbrace{\frac{\partial (\rho \vec{v})}{\partial t}}_{unsteady\ term} + \underbrace{\nabla \cdot (\rho \vec{v} \vec{v})}_{convective\ term} = - \underbrace{\nabla \cdot (\mu \nabla \vec{v})}_{diffusion\ term} + \{\nabla \cdot (\vec{\tau} - \mu \nabla \vec{v}) - \nabla p + \rho \vec{g}\} \tag{4.2}$$

$$\underbrace{\frac{\partial (\rho T)}{\partial t}}_{unsteady\ term} + \underbrace{\nabla \cdot (\rho \vec{v} T)}_{convective\ term} = \underbrace{\nabla \cdot (\frac{\lambda}{c_v} \nabla T)}_{diffusion\ term} + \{\frac{-\nabla \cdot \vec{q}^R - \nabla p \cdot \vec{v} + \vec{\tau} : \nabla \vec{v}}{c_v}\} \tag{4.3}$$

These equations are formed mainly by an unsteady term (which depends on time), a convective term, a diffusive term and other terms (typically named as source terms) [10].

Equation	ϕ	Γ_ϕ	s_ϕ
Mass	1	0	0
Momentum	$\vec{v}$	μ	$\nabla \cdot (\vec{\tau} - \mu \nabla \vec{v}) - \nabla p + \rho \vec{g}$
Energy	T	λ / c_v	$(-\nabla \cdot \vec{q}^R - \nabla p \cdot \vec{v} + \vec{\tau} : \nabla \vec{v})/c_v$

Table 4.1: Navier-Stokes equations into convection diffusion transport form

Hence, for a generic variable ϕ (e.g. velocity, temperature, mass, entropy, etc.) the set of NS equations can be written into a generic convection-diffusion transport equations [11]:

$$\frac{\partial(\rho\phi)}{\partial t} + \nabla \cdot (\rho \vec{v} \phi) = \nabla \cdot (\Gamma_\phi \nabla_\phi) + s_\phi \tag{4.4}$$

where Γ_ϕ is the diffusion coefficient and s_ϕ is the extra source/sink terms.

Using the mass conservation equation, the previous generic convection-diffusion equation can also be written as:

$$\rho \frac{\partial \phi}{\partial t} + \rho \vec{v} \nabla \phi = \nabla \cdot (\Gamma_\phi \nabla_\phi) + s_\phi \tag{4.5}$$

Navier-Stokes equations are solved integrating along time (dt) and space, in this case volume (dV), in the Control Volume (CV).

For the unsteady term:

$$\int_{t_n}^{t_{n+1}} \int_{V_p} \frac{\partial(\rho\phi)}{\partial t} dV \; dt \approx V_p \int_{t_n}^{t_{n+1}} \frac{\partial(\rho\phi)}{\partial t} dt = V_p(\rho_p \phi_p - {\rho_p}^0 {\phi_p}^0)$$

For the convective term:

$$\int_{t_n}^{t_{n+1}} \int_{V_p} \nabla \cdot (\rho \vec{v} \phi) dV \; dt = \int_{t_n}^{t_{n+1}} \int_{S_f} \rho \vec{v} \phi \cdot \vec{n} dS \; dt \approx (\dot{m}_e \phi_e - \dot{m}_w \phi_w + \dot{m}_n \phi_n - \dot{m}_s \phi_s) \triangle t$$

For the diffusion term:

$$\int_{t_n}^{t_{n+1}} \int_{V_p} \nabla \cdot (\Gamma_\phi dV \; dt = \int_{t_n}^{t_{n+1}} \int_{S_f} \Gamma_\phi \nabla \phi \cdot \vec{n} dS \; dt \approx$$

$$\approx (\Gamma_e \frac{\phi_E - \phi_P}{d_{PE}} S_e - \Gamma_w \frac{\phi_P - \phi_W}{d_{PW}} S_w + \Gamma_n \frac{\phi_N - \phi_P}{d_{PN}} S_n - \Gamma_s \frac{\phi_P - \phi_S}{d_{PS}} S_s) \triangle t$$

Finally for the source term (where the source term is supposed lineal):

$$\int_{t_n}^{t_{n+1}} \int_{V_p} s_\phi dV \; dt \approx \bar{s}_{\phi p} V_p \triangle t = (S_C^\phi + S_P^\phi \phi_P) \triangle t$$

Introducing all these terms into the convection-diffusion equation:

$$\frac{\rho_p \phi_p - {\rho_p}^0 {\phi_p}^0}{\triangle t} V_p + \dot{m}_e \phi_e - \dot{m}_w \phi_w + \dot{m}_n \phi_n - \dot{m}_s \phi_s =$$

$$= D_e(\phi_E - \phi_P) - D_w(\phi_P - \phi_W) + D_n(\phi_N - \phi_P) - D_s(\phi_P - \phi_S) + S_C^\phi + S_P^\phi \phi_P \quad (4.6)$$

where $D_e = \Gamma_e S_e / d_{PE}$, $D_w = \Gamma_w S_w / d_{PW}$... An equivalent equation can be obtained using the discretized mass conservation equation:

$$\rho_p \frac{\phi_p - {\rho_p}^0 {\phi_p}^0}{\triangle t} V_p + \dot{m}_e(\phi_e - \phi_p) - \dot{m}_w(\phi_w - \phi_p) + \dot{m}_n(\phi_n - \phi_p) - \dot{m}_s(\phi_s - \phi_p) =$$

$$= D_e(\phi_E - \phi_P) - D_w(\phi_P - \phi_W) + D_n(\phi_N - \phi_P) - D_s(\phi_P - \phi_S) + S_C^\phi + S_P^\phi \phi_P \quad (4.7)$$

These equations are second-order for the diffusion and source term. However, the convective term has to be evaluated in terms of the nodal values, because they are expressed as values at the faces.

4.3 Evaluation of the convective terms

As seen previously, the convective term in Eq.4.7 is evaluated at the face of the CV. However, the values of ϕ are measured at the center of the CV, therefore, an approximation of the value at the faces has to be done. There are several ways of evaluating the convective terms:

4.3.1 Central-Difference Scheme (CDS)

CDS is the simplest method. It can be calculated as the average or using the harmonic mean which takes into account the distance from the nearest nodes to the face.

$$\phi_e - \phi_p = f_e(\phi_E - \phi_P) \quad (4.8)$$

where the interpolation factor is:

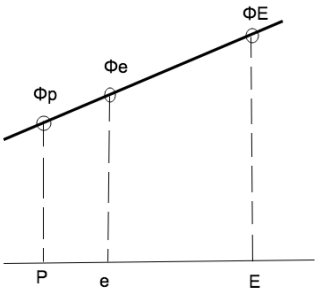

Figure 4.1: Central-Difference Scheme (CDS)

$$f_e = d_{Pe}/d_{PE} \tag{4.9}$$

For the average method, $f_e = 1/2$. Nevertheless, CDS gives convergence problems for incompressible flows, or gases at low Mach, because the convective terms are more influenced by upstream than downstream conditions.

4.3.2 Upwind-Difference Scheme (UDS)

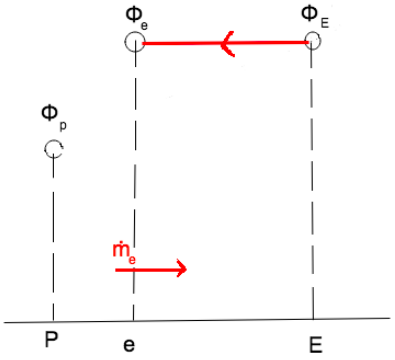

Figure 4.2: Upwind-Difference Scheme (UDS) for $\dot{m}_e > 0$

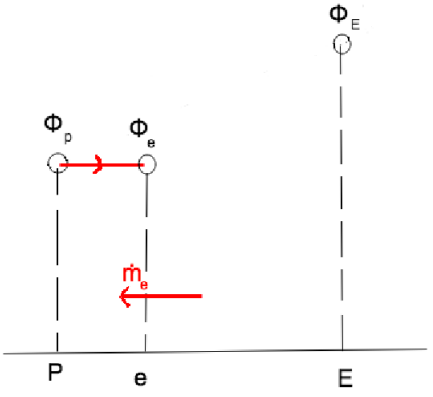

Figure 4.3: Upwind-Difference Scheme (UDS) for $\dot{m}_e < 0$

To solve this problem, UDS method gives more importance to the upstream condition than the downstream.

$$\phi_e - \phi_p = f_e(\phi_E - \phi_P) \tag{4.10}$$

but now:

$$f_e = 1 \quad (if\ \dot{m}_e > 0) \quad and \quad f_e = 0 \quad (if\ \dot{m}_e < 0) \tag{4.11}$$

4.3.3 Exponential-Difference Scheme (EDS)

An analytic solution of the convection-diffusion equation without the source term and for steady conditions can be obtained. Considering ρ, v_x and Γ constants between nodal values and equal to the ones at the face, the equation can be integrated.

For east face:

$$\phi_e - \phi_p = f_e(\phi_E - \phi_P) \tag{4.12}$$

where:

$$f_e = \frac{e^{Pe \cdot d_{Pe}} - 1}{e^{Pe} - 1} \qquad Pe = \frac{\rho_e v_{xe} d_{PE}}{\Gamma_e} \tag{4.13}$$

Finally, the equation to solve in each node has the following structure. The same structure is found for CDS, UDS and EDS schemes.

$$a_p \cdot \phi_p = a_e \cdot \phi_e + a_w \cdot \phi_w + a_n \cdot \phi_n + a_s \cdot \phi_s + b_p \tag{4.14}$$

Where:

$$a_e = f_e \cdot \dot{m}_e - \frac{\Gamma_e}{d_{PE}} S_e \qquad a_w = -f_w \cdot \dot{m}_w - \frac{\Gamma_w}{d_{PW}} S_w$$

$$a_n = f_n \cdot \dot{m}_n - \frac{\Gamma_n}{d_{PN}} S_n \qquad a_s = -f_s \cdot \dot{m}_s - \frac{\Gamma_s}{d_{PS}} S_s$$

$$a_p = a_e + a_w + a_n + a_s - \dot{m}_e + \dot{m}_w - \dot{m}_n + \dot{m}_s \qquad b_p = 0$$

Remember that the coefficients f_e, f_w, f_n and f_s take different values depending on the kind of scheme selected. Regularly, to simplify the nomenclature of the equations new variables are introduced (as named before):

$$F_e = \dot{m}_e \qquad D_e = \frac{\Gamma_n}{d_{PN}} S_n$$

EDS, UDS and CDS are first and second order accurate. Sometimes, it is needed more accurate schemes like a third-order or even higher. The order is related to the number of points consulted in order to establish an approximation of the value at the face.

4.3.4 High-order numerical scheme

- Quadratic Upwind Interpolation for convective kinematics (QUICK)
- SMART
- STOIC
- FROMM
- See more schemes in [12]

In this project, there will be used: QUICK and SMART schemes.

QUICK scheme is a non-linear that consults several nodes along the grid in order to establish a quadratic (x^2) formula to interpolate the value at the face. Moreover, SMART scheme is also non-linear.

The final equation to solve in each grid point has this form:

$$a_p \cdot \phi_p = a_e \cdot \phi_e + a_w \cdot \phi_w + a_n \cdot \phi_n + a_s \cdot \phi_s + b_p \tag{4.15}$$

In this case, the coefficients of discretization are different:

$$a_e = D_e - \frac{\dot{m}_e - |\dot{m}_e|}{2} \qquad a_w = D_w + \frac{\dot{m}_e + |\dot{m}_e|}{2}$$

$$a_n = D_n - \frac{\dot{m}_n - |\dot{m}_n|}{2} \qquad a_s = D_s + \frac{\dot{m}_s + |\dot{m}_s|}{2}$$

$$a_p = a_e + a_w + a_n + a_s + \frac{\rho_P^0 V_p}{\Delta t} - S_p^\phi V_p$$

$$b_p = \frac{\rho_P^0 V_p}{\Delta t}\phi_P^0 + S_c^\phi V_p - \dot{m}_e(\phi_e^{HRS,*} - \phi_e^{UDS,*}) + \dot{m}_w(\phi_w^{HRS,*} - \phi_w^{UDS,*})...$$
$$-\dot{m}_n(\phi_n^{HRS,*} - \phi_n^{UDS,*}) + \dot{m}_s(\phi_s^{HRS,*} - \phi_s^{UDS,*})$$

The source term is linearized as $\bar{s}_{\phi P} = S_C^\phi + S_P^\phi \phi_P$. And $\phi_e^{HRS,*}$ and $\phi_e^{UDS,*}$ are the values at the corresponding face using a high order scheme (HRS) and Upwind scheme (UDS) respectively calculated at the previous iteration.

4.4 Convection-Diffusion problems

In this section, there have been developed some proposal exercises. The following exercises are steady and bidimensional, velocity field is known and density and diffusion coefficients are known constant values.

4.4.1 Parallel flow

The first problem to solve is a parallel flow in a duct of a rectangle domain (LxH) with the following particularities and boundary conditions:

- The velocity field is kwown: $v_x = v_0$ and $v_y = 0$.
- Inlet conditions (x=0,y): ϕ=ϕ_{in};
- Outlet conditions (x=L,y): ϕ=ϕ_{out};
- Lateral conditions (x,y = 0):$\partial\phi/\partial y = 0$.

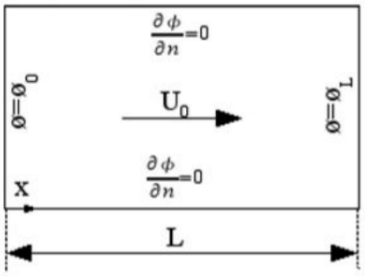

Figure 4.4: Parallel flow : First Convection-Diffusion problem

In order to observe how the obtained solution varies for different physical parameters, the solution will be tested for different Péclet numbers (Eq. 4.16).

The Péclet number (Pe) is a dimensionless number, that computes the ratio of the rate of advection of a physical quantity by the flow to the rate of diffusion of the same quantity driven by an appropriate gradient [10].

$$Pe = \frac{Advective\ \ transport\ \ rate}{Diffusive\ \ transport\ \ rate}$$

For heat transfer, the Péclet number is defined as:

$$Pe = \frac{L \cdot u}{\alpha} = Re_L \cdot Pr \qquad Pe = \frac{\rho v_0 L}{\Gamma} \tag{4.16}$$

where Pr is the Prandtl Number and Re is the Reynols Number.

An analytical solution (Eq.4.17) can be obtained [10]. Consecutively, the results obtained will be compared with the analytic solution.

$$\frac{\phi - \phi_{in}}{\phi_{out} - \phi_{in}} = \frac{e^{xPe/L} - 1}{e^{Pe} - 1} \tag{4.17}$$

A program has been developed *CD-ParallelFlow.cpp* (Code in *Annex II*) to solve this problem. The solution for different Péclet numbers (-20, -10, -5, -1, 0 ,1, 5, 10, 20) are collected in Figure 4.5:

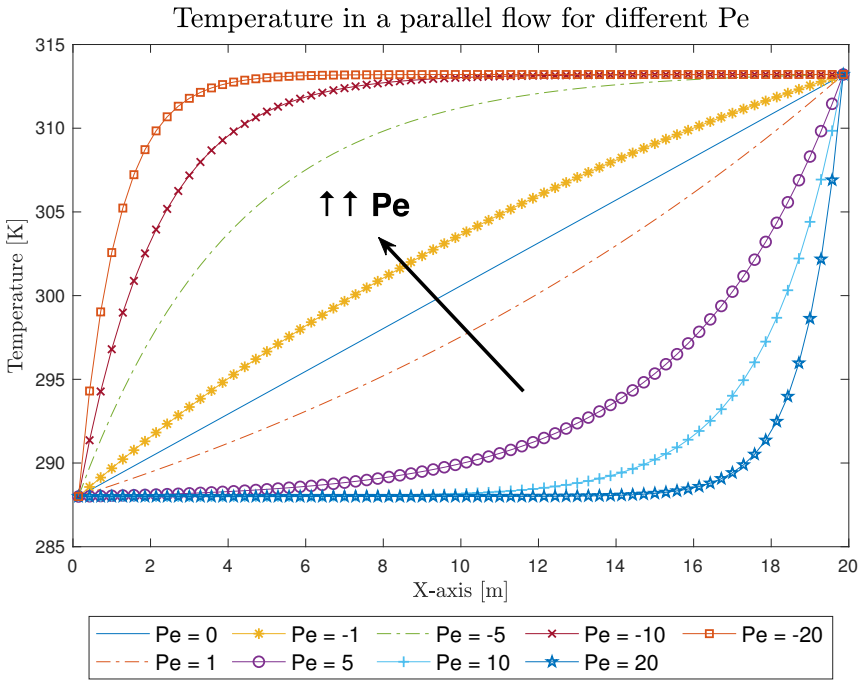

Figure 4.5: Temperature along X-axis for different Péclet numbers

The maximum error found for Pe=1 using different schemes in a grid point is approximately 0.4 %. So the solution obtained can be considered as consistent.

Fistly, the problem has been solved as a one-dimensional (1D) problem in order to ensure that the calculations of the coefficients, parameters and the results obtained are correct. The same code has been increased to bidimensional (2D) to solve this problem and the following.

On the other hand, in Figure 4.6 the solutions obtained with CDS, UDS, EDS, QUICK and SMART schemes have been plotted for Pe = 1. The difference between them is negligible for this Péclet number.

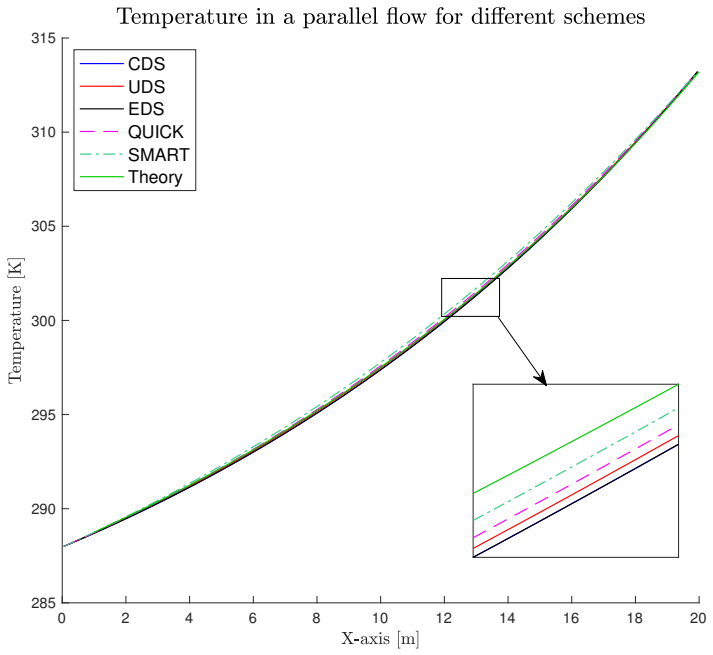

Figure 4.6: CDS , UDS, EDS, QUICK & SMART solutions for Pe = 1

4.4.2 Diagonal flow

In this case, the domain is a square (LxL) and the velocity field is known (Eq.4.18):

$$v_x = v_o \cdot sin(\alpha) \qquad v_x = v_o \cdot sin(\alpha) \tag{4.18}$$

For $v_o = 30\sqrt{2}$ and $\alpha = 45^o$, the velocity field is: $v_x = 30$; $v_y = 30$.

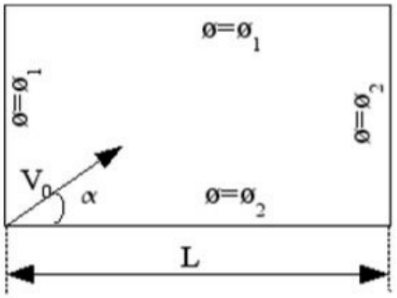

Figure 4.7: Diagonal Flow : Second Convection-Diffusion problem

For number Pe=0.6, the following solution has been obtained with UDS method Figure 4.8. A program has been developed to obtain the solution *CD-Diagonal.cpp* (Code in *Annex II*).

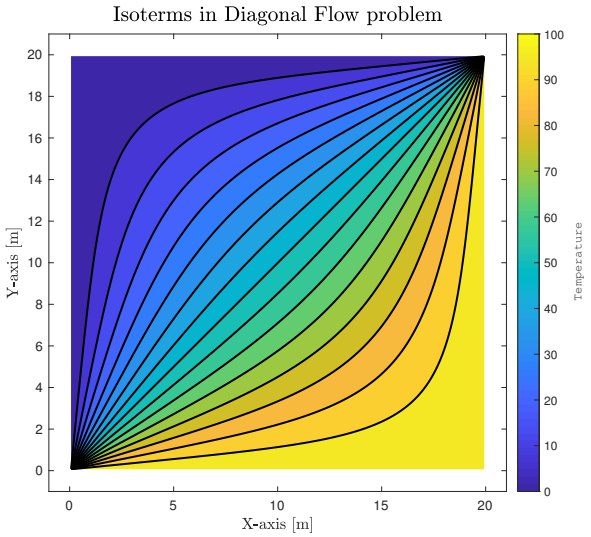

Figure 4.8: Isotherms in a Diagonal Flow (Pe=0.6)

In Figure 4.8, the isotherms are plotted. It can be observed that the value of temperature along the domain depends on the influence of the nearest boundary conditions. The value of the main diagonal is $\frac{\phi_{HIGH}+\phi_{LOW}}{2}$. A symmetrical behaviour is observed in this case.

Furthermore, for Pe $= \infty$ using UDS method a solution has been obtained in Figure 4.9. As observed, the solution can be divided into two regions. The upper diagonal part in which the temperature (ϕ) achieves the value of ϕ_{LOW} and the lower diagonal part, the temperature corresponds to ϕ_{HIGH}.

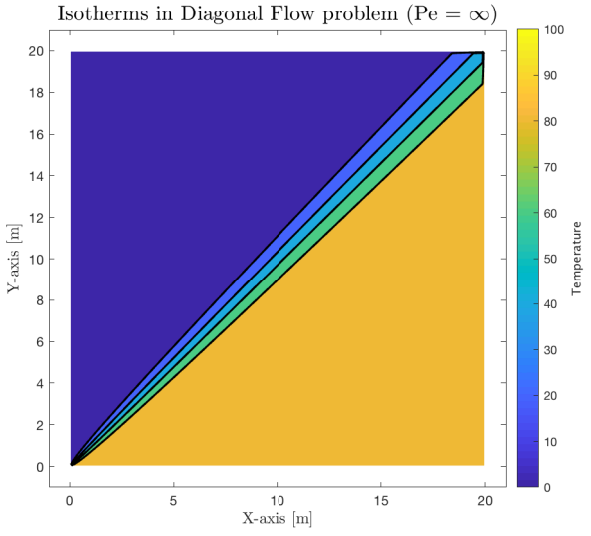

Figure 4.9: Isotherms in a Diagonal Flow ($Pe = \infty$)

4.4.3 Smith-Hutton problem

This problem was proposed by R.M. Smith and A.G. Hutton in 1982. Smith-Hutton problem is a test problem which permits the evaluation of different numerical schemes (first order, second order, third or higher orders).

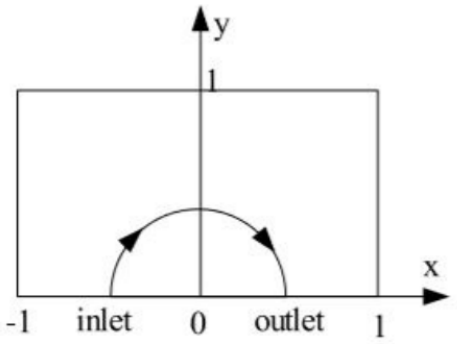

Figure 4.10: Smith-Hutton problem : Third Convection-Diffusion problem

The problem consists in a rectangular region (2LxL), with one inlet and one outlet [13]. The stream function Ψ is known (Eq.4.19), therefore the velocity field of the fluid is also known (Eq.4.20).

$$\Psi = (1 - x^2) \cdot (1 - y^2) \tag{4.19}$$

$$u(x,y) = \frac{\partial \Psi}{\partial y} = 2y(1 - x^2) \qquad v(x,y) = -\frac{\partial \Psi}{\partial x} = -2x(1 - y^2) \tag{4.20}$$

All boundary conditions are Dirichlet, except for the boundary at the outlet wall that is Neummann boundary condition.

$$\phi = 1 + tanh(\alpha(2x + 1)) \qquad (for\ y = 0;\ -1 < x < 0) \quad (Inlet flow)$$

$$\frac{\partial \phi}{\partial y} = 0 \qquad (for\ y = 0;\ 0 < x < 1) \quad (Outlet\ flow)$$

$$\phi = 1 + tanh(\alpha) \qquad (for\ the\ rest\ of\ walls)$$

In this case, $\alpha = 10$. The solution has been done for different ratios of ρ/Γ (10, 10^3, 10^6) and with different schemes (CDS, UDS, EDS and higher order schemes). A program has been developed to obtain the solution *CD-SmithHutton.cpp* (Code in *Annex II*).

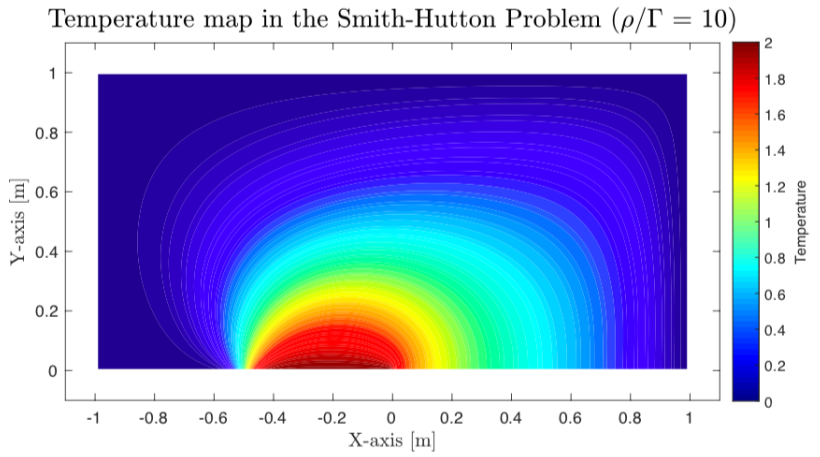

Figure 4.11: Solution of Smith-Hutton problem for Pe = 10

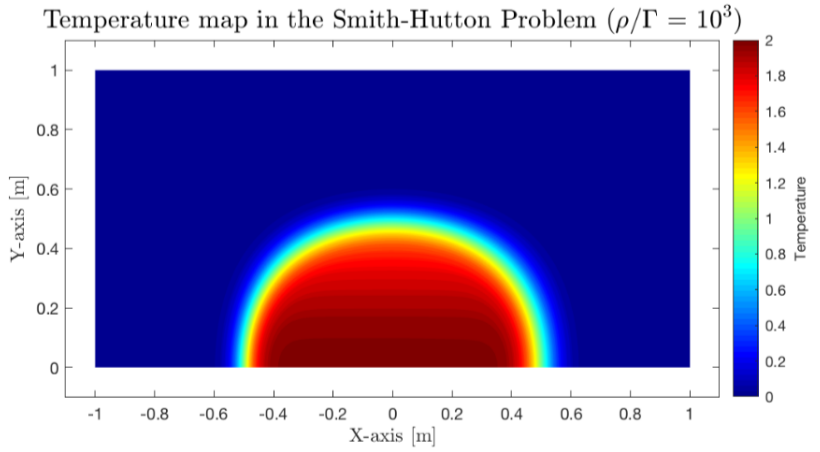

Figure 4.12: Solution of Smith-Hutton problem for Pe = 10^3

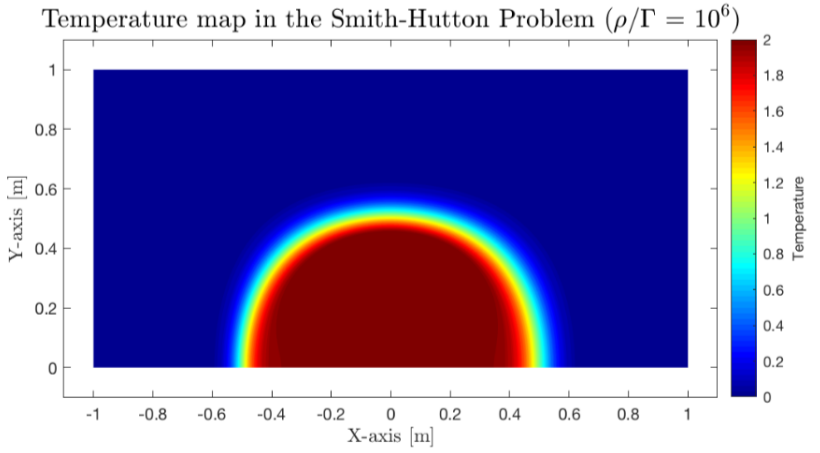

Figure 4.13: Solution of Smith-Hutton problem for Pe = 10^6

	$\rho/\Gamma = 10$		$\rho/\Gamma = 10^3$		$\rho/\Gamma = 10^6$	
x-position	ϕ_{theo}	ϕ_{exp}	ϕ_{theo}	ϕ_{exp}	ϕ_{theo}	ϕ_{exp}
0.0	1.989	1.988	2.0000	2.0000	2.000	2.000
0.1	1.402	1.442	1.9990	1.9992	2.000	2.000
0.2	1.146	1.210	1.9997	1.9983	2.000	2.000
0.3	0.946	0.964	1.9850	1.9955	1.999	2.000
0.4	0.775	0.781	1.8410	0.9737	1.964	1.983
0.5	0.621	0.632	0.9510	0.9737	1.000	0.959
0.6	0.480	0.501	0.1540	0.0950	0.036	0.089
0.7	0.349	0.352	0.0010	0.0024	0.001	0.002
0.8	0.227	0.225	0.0000	0.0000	0.000	0.000
0.9	0.111	0.107	0.0000	0.0000	0.000	0.000
1.0	0.000	0.000	0.0000	0.0000	0.000	0.000

Table 4.2: Comparison between obtained results for different $\frac{\rho}{\Gamma}$ ratios

In Table 4.2, the values at the outlet wall for several x-positions and for different ρ/Γ ratios are compared with the results from the reference data [14].

For ρ/Γ=10, the solution obtained has a broad range of temperatures. It can be observed that the value of T is transported by the motion of the flow (Eq.4.20), for ρ/Γ=10 case CDS was used.

Nevertheless, for ρ/Γ=10^3 and ρ/Γ=10^6 a different behaviour is observed. The flow is prone to follow the direction of the velocity field and the diffusion is mitigated strongly. For these cases, a symmetrical behaviour is observed, but not for ρ/Γ=10. For these cases, CDS is not working correctly and it does not converge, so UDS and QUICK were used to obtain the solution.

Different numerical schemes are needed for particular cases, some of them work perfectly for Pe < 2, such as CDS, however for higher Pe, a higher order scheme is compulsory.

4.5 Convection-Diffusion resolution

In order to solve Convection-Diffusion incompressible and steady problems the sequence of actions and calculations are resumed in Figure 4.14.

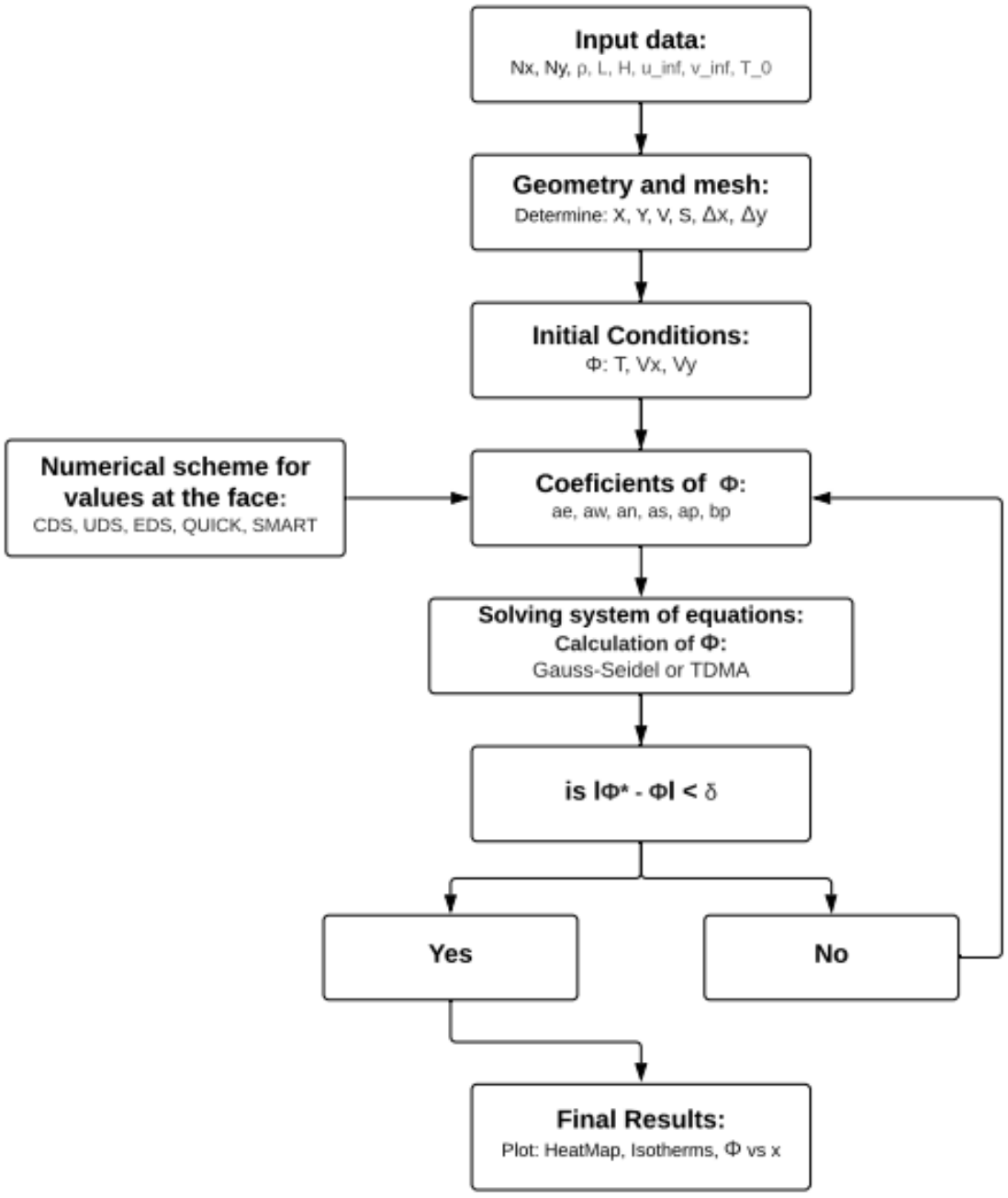

Figure 4.14: Diagram solution of steady Convection-Diffusion problems

4.6 Summary

In this chapter, there have been developed several convection-diffusion steady and bidimensional problems, in which velocity field is known and density and diffusion coefficients are known as constant values.

One of the main aspects in this chapter was to select a suitable scheme to guess the value of ϕ at the face. In the mesh, the values of ϕ are held in the middle of CV. However, in momentum equation the terms of mass flux are calculated with the values at the face.

There are several schemes (CDS, UDS, EDS, SMART...), some of them are first-order, second-order or even higher. The order depends on the number of points the scheme checked to guess the value of ϕ. In problem *4.4.2 Diagonal flow* and *4.4.3 Smith-Hutton problem* schemes take an important role in the obtainment of the solution. For first-order schemes and high Pe, the solution does not converge.

In the problem *Parallel flow*, it can be observed that Pe number has an important role on the solution. Péclet number defines the ratio between the convective and the diffussion terms. The higher the Pe, the stronger convection terms are, so the value of a physical property transported along the direction of the flow will be prone to maintain its value with the distance travelled. Moreover, no loss or dissipation would happen.

Finally, *Smith Hutton problem* is the suitable problem to test the numerical scheme used. In this case, the convergence of the solution depends on the ratio ρ/Γ and the scheme selected. For high ratios, a second or third order scheme is compulsory.

5 Navier-Stokes

On this chapter there will be developed a solution of Navier-Stokes for the Driven Cavity case using Fractional Step Method (FSM).

5.1 Introduction

The Navier-Stokes equations consist of a set of time dependent equations: continuity of mass (1 equation), conservation of momentum (3 equations: x, y, z) and energy conservation (1 equation).

As seen in previous chapters, some terms in the equations are responsible of the convection (physical process inside a fluid where a property is transported by the ordered motion of the flow) and of diffusion (physical process physical process that occurs in a flow of gas in which some property is transported by the random motion of the molecules of the gas)[9].

All equations are dependent in each other, so to solve all the equations in a flow problem, the five equations have to be solved simultaneously. There are actually other equations that are required to solve this system such as an equation of state that relates the pressure, temperature, and density of the gas ($P = \rho RT$).

In the following section, FSM will be used in order to obtain a numerical resolution of the Navier-Stokes equations.

5.2 Fractional Step Method (FSM)

Fractional Step Method (FSM) is common technique for solving incompressible NS equations. The Navier-Stokes equations (Eq.5.1 and Eq.5.2) for incompressible and constant viscosity flows are :

$$\nabla \cdot (\rho \vec{v}) = 0 \tag{5.1}$$

$$\rho \frac{\vec{v}}{\partial t} + (\rho \vec{v} \cdot \nabla)\vec{v} = -\nabla p + \mu \nabla \vec{v} \tag{5.2}$$

Introducing the new term R, the momentum equation can be written as:

$$\rho \frac{\vec{v}}{\partial t} = \mathbf{R}(\vec{v}) - \nabla p \tag{5.3}$$

where, $\mathbf{R}(\vec{v}) = -(\rho \vec{v} \cdot \nabla)\vec{v} + \mu \nabla \vec{v}$.

Time intregration of NS equations are:

$$\nabla \cdot (\rho \vec{v}^{n+1}) = 0 \tag{5.4}$$

$$\rho \frac{\vec{v}^{n+1} - \vec{v}^{n}}{\delta t} = \frac{3}{2}\mathbf{R}(\vec{v}^{n}) - \frac{1}{2}\mathbf{R}(\vec{v}^{n+1}) - \nabla p^{n+1} \tag{5.5}$$

For time integration of the convective-diffusive term Adams-Bashforth scheme is used.

Momentum equations are integrated at time instant (n+1/2) while continuity equations is implicitly integrated.

Now, it will be introduced a unique decomposition (thanks to the Helmholtz-Hodge theorem).

5.2.1 Helmholtz-Hodge theorem

The theorem establishes that a given A and given vector field ω, defined in a bounded domain Ω with smooth boundary $\Delta\Omega$, is uniquely decomposed in a pure gradient field and a divergence-free vector parallel to $\Delta\Omega$.

$$\vec{\omega} = \vec{a} + \nabla\phi$$

where, $\nabla\vec{a} = 0$ for a Ω. The theorem also applies for periodic inflow/outflow conditions.

Introducing the HH theorem into Eq.5.3, an equation for pressure can be derived from the velocity decomposition equations if the divergence operator is applied:

$$\nabla\vec{v}^{n+1} = \nabla\vec{v}^{p} - \nabla \cdot (\frac{t}{\rho}\nabla p^{n+1})$$

Since $\nabla\vec{v}^{n+1} = 0$, finally a Poisson equation for the pressure is found:

$$\nabla p^{n+1} = \frac{\rho}{t}\nabla \cdot \vec{v}^{p}$$

Finally, v^{n+1} results from the original decomposition:

$$\vec{v}^{n+1} = \vec{v}^{p} - \frac{t}{\rho}\nabla p^{n+1}$$

Hence, at each time step the following equations give a unique $\vec{v}^{n+1}$ and ∇p^{n+1}. The FSM can be resumed in these steps:

1. Evaluation of $\mathbf{R}(\vec{v})^n)$
2. Evaluate the predictor velocity $(\vec{v})^p)$, using the convective-diffusive temrs of the previous step: $(\vec{v})^p) = (\vec{v})^n) + \frac{t}{\rho}[3/2\mathbf{R}(\vec{v})^n) - 1/2\mathbf{R}(\vec{v})^{n+1})]$
3. Solve Poisson equation to obtain the pressure: $\nabla p^{n+1} = \frac{\rho}{t}\nabla\vec{v}^p$
4. Obtain the velocity field: $\vec{v}^{n+1} = \vec{v}^p - \frac{t}{\rho}\nabla p^{n+1}$
5. Choose the new t = min (t_c,t_d)

The predictor velocity provides an approximate solution of the momentum equations, but it cannot satisfy the incompressibility constraint. The Poisson equation for pressure [15] determines the minimum perturbation that will make the predictor velocity incompressible.

5.2.2 Checkerboard problem

A checkerboard problem arises due to the nature of the central difference scheme when applied to the divergence operator and the pressure gradient operator.

The calculation of the pressure gradient only depends on the pressure surrounding nodes, but not the node it self. This could give unrealistic pressure fields, even though a realistic and stable velocity field is obtained.

There are two possibilities to solve this problem:

- Collocated mesh

  In the collocated mesh in Cartesian coordinates velocity components (u, v, w) are stored with the pressure p at the cell centre [16].

  An interpolation of the velocity value at the wall has to be interpolated through interpolation of the cell-centered values plus a projection operation that guarantees exact conservation of mass [17].

- Staggered mesh

  In a staggered mesh, one mesh is created for the pressure field and another for the velocity field [16, 18]. In this case, for velocity field $\vec{v}$ = (u , v) it will be used a staggered mesh in order to avoid the checkerboard problem.

  On a staggered grid the scalar variables (pressure, density, total enthalpy etc.) are stored in the cell centres of the control volumes, whereas the velocity or momentum variables are located at the cell faces. A staggered storage is mainly used on structured grids for compressible or incompressible flow simulations.

Using a staggered grid (Figure 5.1) is a simple way to avoid odd-even decoupling [19] between the pressure and velocity. Odd-even decoupling is a discretization error

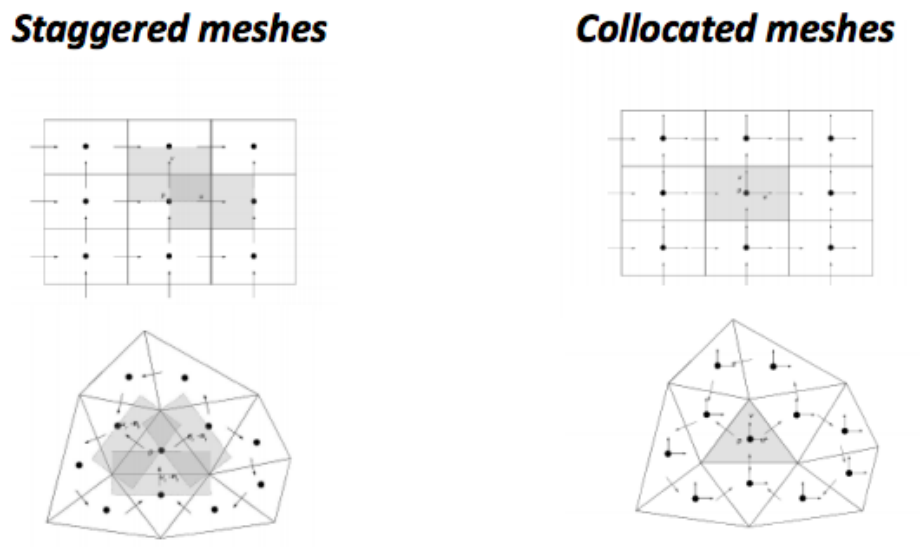

Figure 5.1: Collocated and Staggered Meshes

that can occur on collocated grids and which leads to checkerboard patterns in the solutions.

The disadvantage of using staggered grids is that different variable are stored at different places and this makes it more difficult to handle different control volumes for different variables and to keep track of the metrics. Most modern codes instead use a collocated storage. [20]

The FSM is used at each time step and finishes when the steady state is reached.

5.3 Time step determination

According to CFL (Courant-Friedrich-Levy) condition, the minimum time for convective and for diffusive term are:

$$t_c = min(0.35\ \frac{x}{\vec{v}}) \tag{5.6}$$

$$t_d = min(0.20\ \frac{\rho x^2}{\mu}) \tag{5.7}$$

$$t = min(t_c, t_d) \tag{5.8}$$

5.4 Navier-Stokes problems

In this section, there has been developed the solution for Driven Cavity problem in which NS equations will be solved for a viscous fluid. Theis case was previously solved by scientists and researchers, so there is reference data to check the solution.

5.4.1 Driven Cavity

The Driven Cavity problem (also known as lid-driven cavity), is a NS problem used to test the codes and solution methods to solve Navier-Stokes equations. It consists in a two dimensional (2D) cavity with a viscous flow inside. The cavity is a square whose top wall is moving with constant velocity (u), and the other walls are fixed.

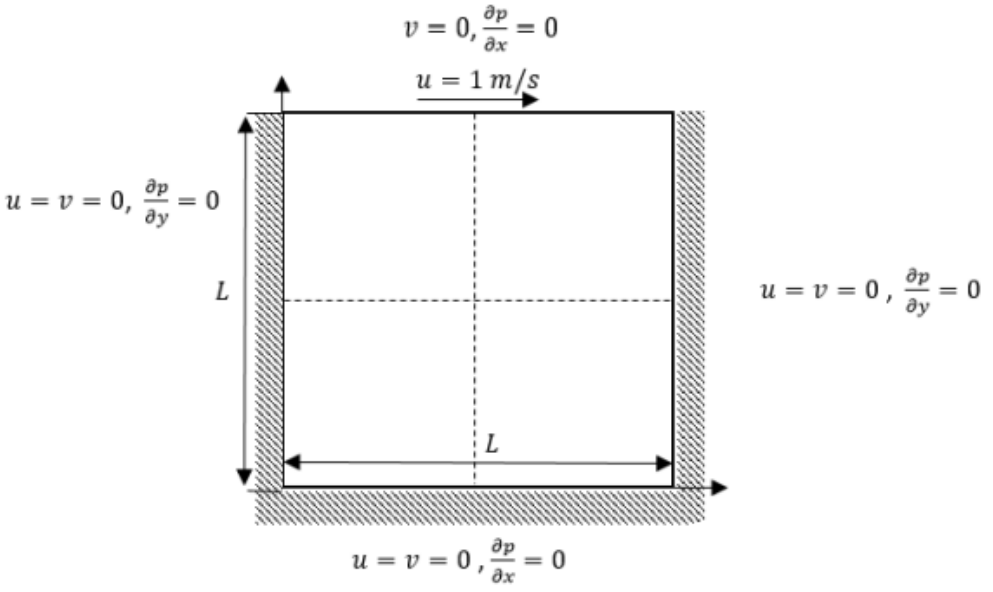

Figure 5.2: Driven Cavity problem

There has been developed a program *NS-DrivenCavity.cpp* (Code in *Annex III*) to solve this problem for different Re. In the report, Re=100 and Re=1000 are only included. However, in *Annex III* there have been included the solution for Re=100, Re=400, Re=1000, Re=5000.

Reynolds number (Re) is a ratio of the an important dimensionless number in fluid mechanics used to help predict flow patterns in different fluid flow situations [21].

$$Re = \frac{inertial\ forces}{viscous\ forces} \tag{5.9}$$

5.4.1.1 Driven Cavity for Re=100

For Re=100 and a structured mesh of dimension 40x40 the following solutions have been obtained. In Figure 5.3 and Figure 5.4, there has been plotted the velocity of the grid points in x-direction and y-direction, respectively. Figure 5.5 corresponds to the pressure in the domain while in Figure 5.5 the module of the velocity has been represented.

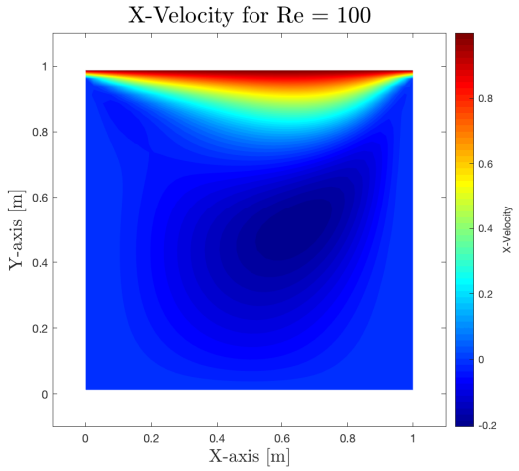

Figure 5.3: X-velocity for Re=100

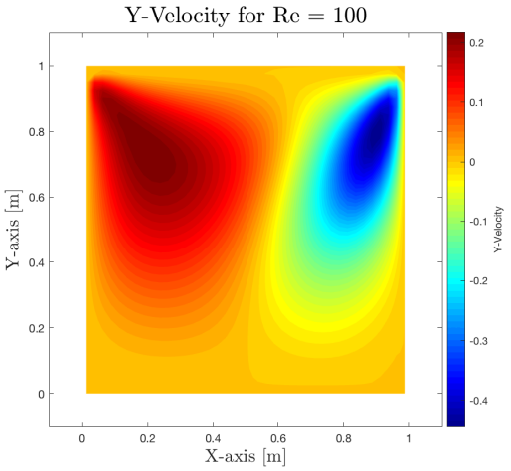

Figure 5.4: Y-velocity for Re=100

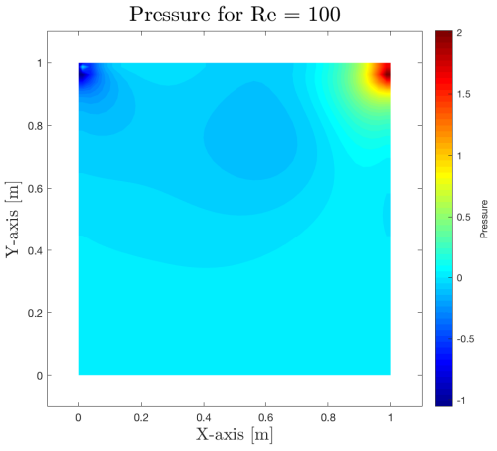

Figure 5.5: Pressure for Re=100

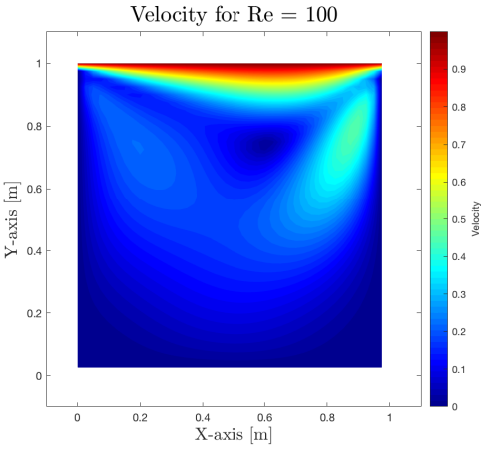

Figure 5.6: Velocity for Re=100

In Figure 5.3, it can be observed that highest velocity is found at the top of the domain and high pressure is found at the top-east corner where the inlet flow is impacting (Figure 5.5).

A vortex seems to be formed in upper middle part of the cavity, lower middle part seems to be still with no flow movement.

In Figure 5.7, there has been represented the velocity in x-direction for the vertical line at the centre of the domain for different dimensions of the mesh compared with the solution obtained in [22], and in Figure 5.8, the velocity in y-direction for a horizontal line at the centre of the domain, respectively for different sizes of the mesh.

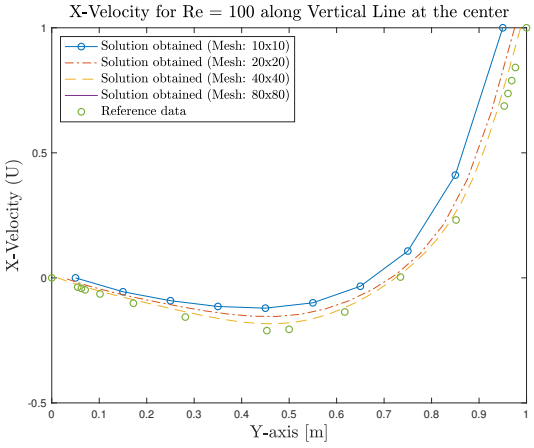

Figure 5.7: X-velocity for Re=100 along a vertical line at the centre of the domain

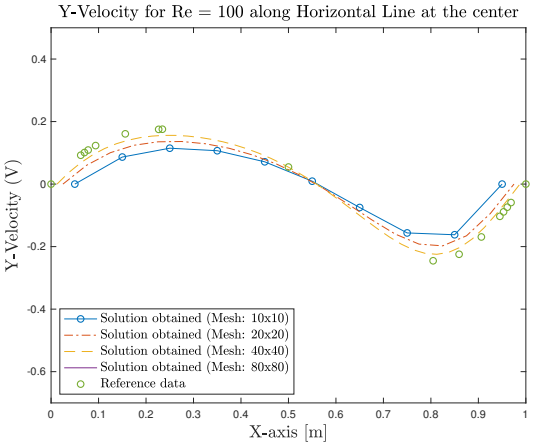

Figure 5.8: Y-velocity for Re=100 along a horizontal line at the centre of the domain

5.4.1.2 Driven Cavity for Re=1000

For Re=1000 and for a mesh of dimension 130x130, the following solutions have been obtained. In Figure 5.9 and Figure 5.10, there has been plotted the velocity of the grid points in x-direction and y-direction, respectively. Figure 5.11 corresponds to the pressure in the domain while in Figure 5.11 the module of the velocity has been represented.

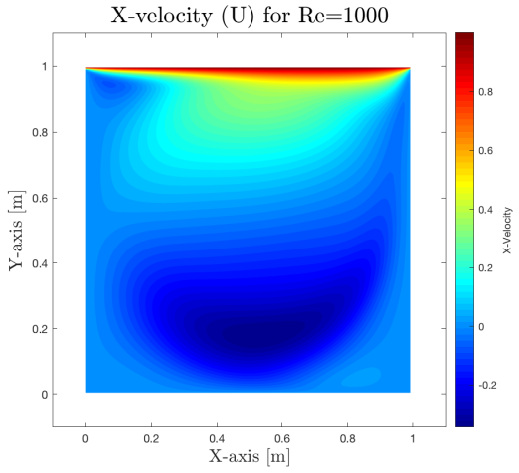

Figure 5.9: X-velocity for Re=1000

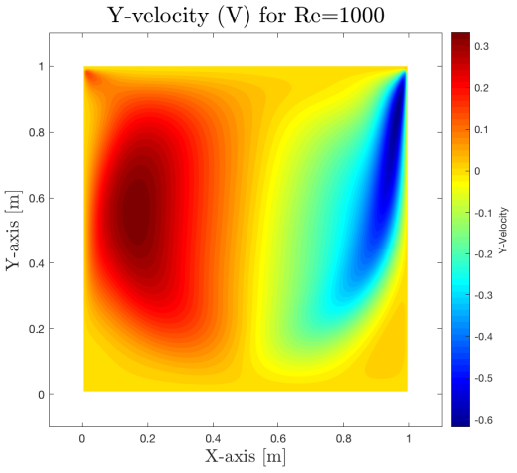

Figure 5.10: Y-velocity for Re=1000

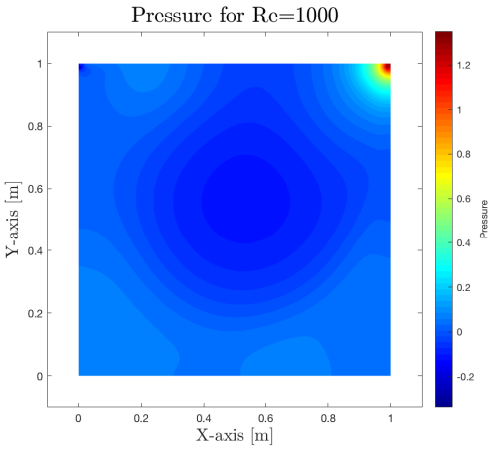

Figure 5.11: Pressure for Re=1000

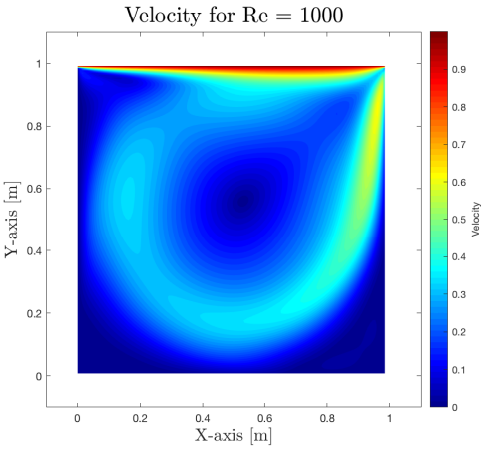

Figure 5.12: Velocity for Re=1000

In Figure 5.9 and in Figure 5.12, it can be observed that highest velocity is found at the top of the domain. Also noted that in Figure 5.11 a high pressure zone is formed at the top-east corner and a low pressure zone in the middle. In Figure 5.12, can be observed that is forming a big vortex in the middle of the square in clockwise direction.

In Figure 5.13, there has been represented the velocity in x-direction for the vertical line at the centre of the domain for different dimensions of the mesh compared with

the solution obtained in [22], and in Figure 5.14, the velocity in y-direction for a horizontal line at the centre of the domain, respectively. It can be observed that the higher the density of the mesh, the more accurate is the answer compared to the reference data.

For a mesh 130x130, the results are practically the same as reference, in spite of the computational time is tremendous.

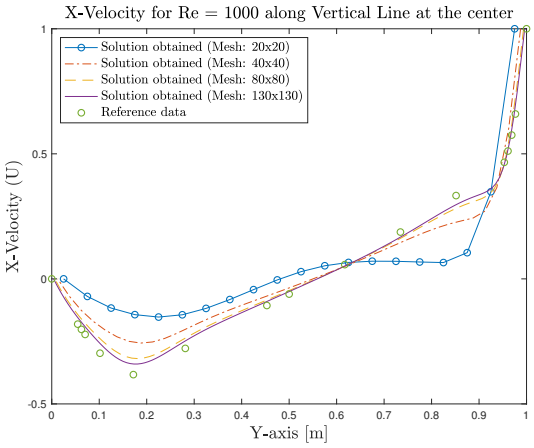

Figure 5.13: X-velocity for Re=1000 along a vertical line at the centre of the domain

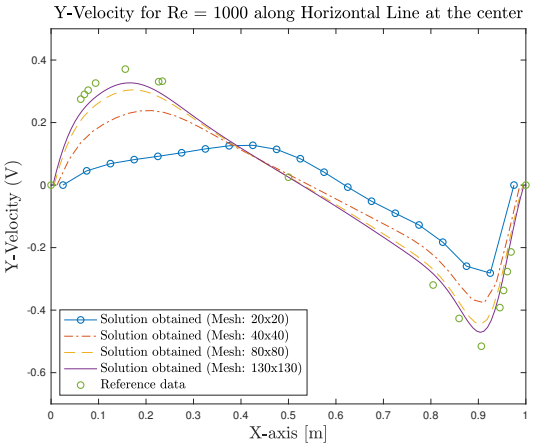

Figure 5.14: Y-velocity for Re=1000 along a horizontal line at the centre of the domain

5.5 Navier-Stokes resolution

The procedure to solve the problem is shown in Figure 5.15. First of all, the mesh and its geometry are determined and the initial conditions (for velocity and pressure in this case) are set.

In order to start the solution, the first time step update is done and FSM function (process described in section *Fractional Step Method (FSM)*) is entered to obtain a velocity field that provides a realistic solution for the pressure field calculated.

Sequentially, the coefficients (a_e, a_w, a_n, a_s, a_p and b_p) are calculated and the system of equations is solved. Then, the convergence is checked and if the solution achieved satisfies the convergence criterion, a new time step is introduced. Next step is to do again the time step update and to repeat the process (remember that time step introduced is given by Eq.5.8). Once the time accumulated is the final established time or the steady state is reached, the final results are saved.

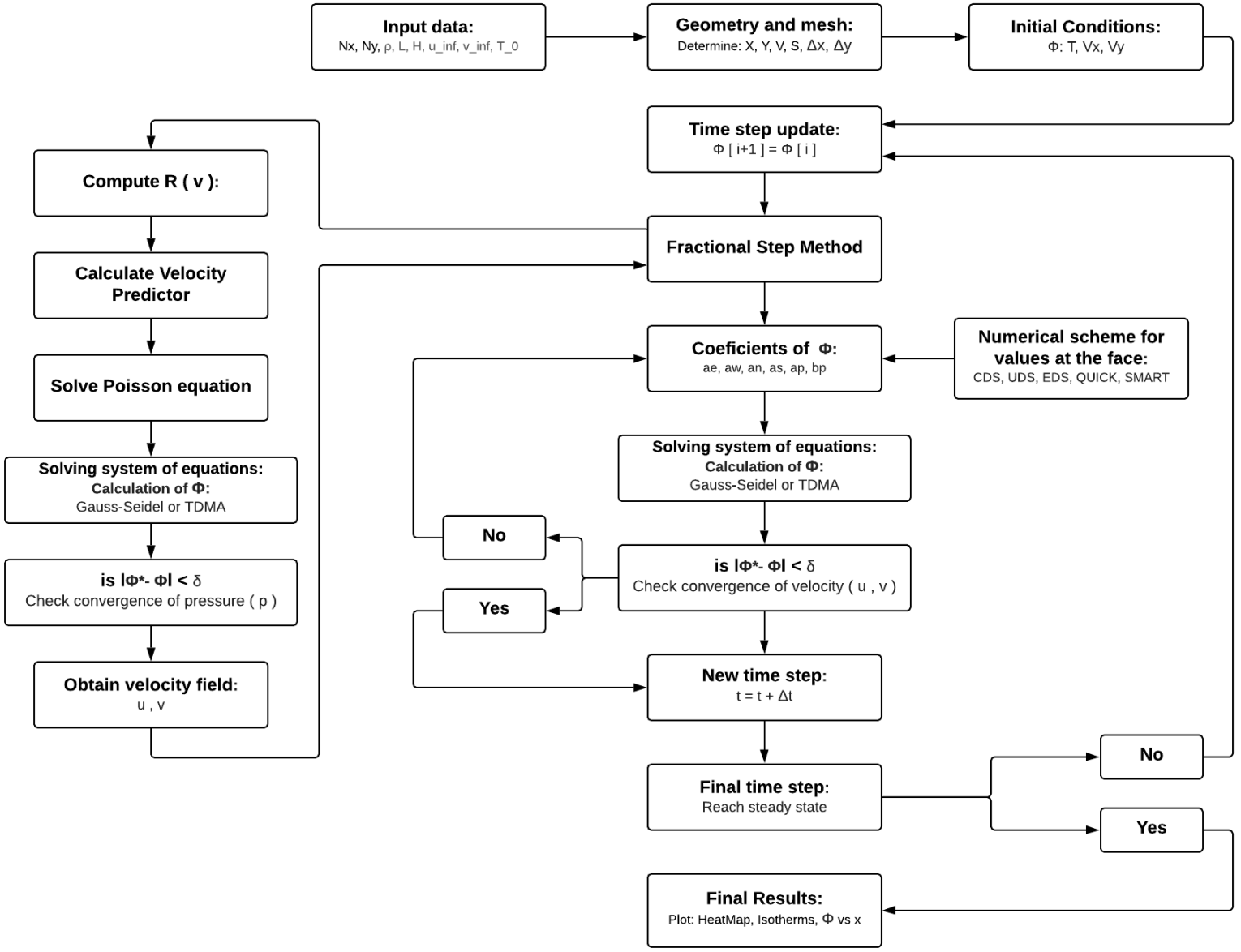

Figure 5.15: Procedure of the resolution of Driven Cavity problem

5.6 Summary

In this chapter, there have been developed the solutions for Driven Cavity problem for different Re. In this case, neither the components of velocity nor the pressure were known, therefore a computation of each term was needed.

Fractional Step Method (FSM) was used to solve incompressible NS equations. The first step was to evaluate the term R, for then evaluate the velocity predictor that enables to solve Poisson equation. Next step was to obtain the velocity field obtained with the previously calculated pressure field.

As seen in *5.2.2 Checkerboard problem*, different structured meshes were used for each variable: one mesh for the pressure, one for velocity in x-direction and other for velocity in y-direction (Staggered meshes). Staggered meshes solve the possibility of achieving a realistic and stable velocity field, but with an unrealistic pressure field.

For Re=100, the highest values of velocity field were obtained mainly in the top region where the inlet flow is, little interaction seems to happen with the rest of the viscous flow.

Nevertheless, for Re=1000 a big vortex in clockwise direction is formed in the middle of the cavity as seen in Figure 5.12. One important fact is the number of divisions that each case needs to be the desired value. For Re=100, a mesh of 20x20 is adequate to achieve results close enough to reference data, although for Re=1000 a mesh of size 80x80 is needed to get a acceptable result comparing with reference data.

It is clearly observed that Reynolds number (Re) has an important role in the solution and in the computational time needed to obtain it. For higher Re, the size mesh needs to be higher and consequently running time is increasing significantly.

To illustrate this fact, for example the computational time for Re=100 with a mesh of 40x40 was 10.323 sec and the virtual time is 5.744 sec (Virtual time is the time needed for achieving steady state). Whereas, for Re=1000 with a mesh 40x40 is 15.899 sec and for a virtual time of 37.543 sec, even though the solution obtained is not as close to reference data as it is for Re=100, so a more dense mesh would be inevitable. Finally, for a mesh 130x130 for Re=1000, the computational time is 548.952 sec (9.15 minutes) and virtual time is 82.570 sec.

6 Economic, environmental study impact and scheduling

In this section, the environmental and economic impact of the project *Computational studies of non-viscous and viscous fluid flows* are determined.

6.1 Economic impact analysis

The economic impact analysis is developed with more detail in the document *Bugdet*. The Table 6.1 summarises the final costs obtained in *Budget*.

	Price [€]
Human costs	7,400.00
Hardware costs	105.00
Electricity costs	10.00
Software costs	70.00
Printing and binding	50.00
Total price	**7,635.00**

Table 6.1: Total costs

6.2 Environmental impact analysis

In this section, it will developed the impact that the project had in the environment. During the elaboration of the project, the only material used were a laptop and several sheets of paper.

In order to find the ecological footprint emitted in the developing of this project. In order to know the power consumption of the used laptop, in this case *MacBook Air (13-inch, Mid 2011)* with a processor 1,8 GHz Intel Core i7 and memory 4 GB 1333 MHz DDR3.

The power for a voltage of 220 V and an intensity 1 A, therefore the power is 220 W = 0.220 kW (P = V · I) (Specs consulted in [23]).

Once known the power consumption, the kg of CO_2 emitted to the environment can be calculated. According to *Red Eléctrica de España*, last year 2018 the average of tones of CO_2 produced by MWh was 0.276 (276 g/kWh) [24].

Thus, supposing that the number of hours using the computer are around 350 h; the number of kg of CO_2 produced are:

$$kg\ of\ CO_2 = 350\ h \cdot 0.220kW \cdot 276\frac{g}{kWh} = 21,252g\ of\ CO_2 \approx 21kg\ of\ CO_2 \quad (6.1)$$

As seen, CO_2 are relatively low. Furthermore, CFD programming codes offer the possibility to run simulations of physical problems without running experimental simulations (such as wind tunnel tests) which are more expensive and obviously the environmental impact is much higher.

6.3 Scheduling

In this section, there will be commented how the project was scheduled. Figure 6.1 corresponds to the Diagram of Gantt developed in *Project Charter*, the tasks of the study are mentioned chronologically.

The first tasks correspond to *Potential Flow* and the schedule went as programmed. However, *Convection-Diffusion* took more time than the expected. Numerical schemes were needed in this chapter, and they were difficult to compute.

Finally, Navier-Stokes case implying turbulence was solved with Driven-Cavity problem. All tasks were completed, nevertheless the time estimation done at the beginning was not followed very carefully.

Developing the report, budget and annexes were also tasks that were not calculated correctly beforehand. They were totally underestimated and took more time than expected.

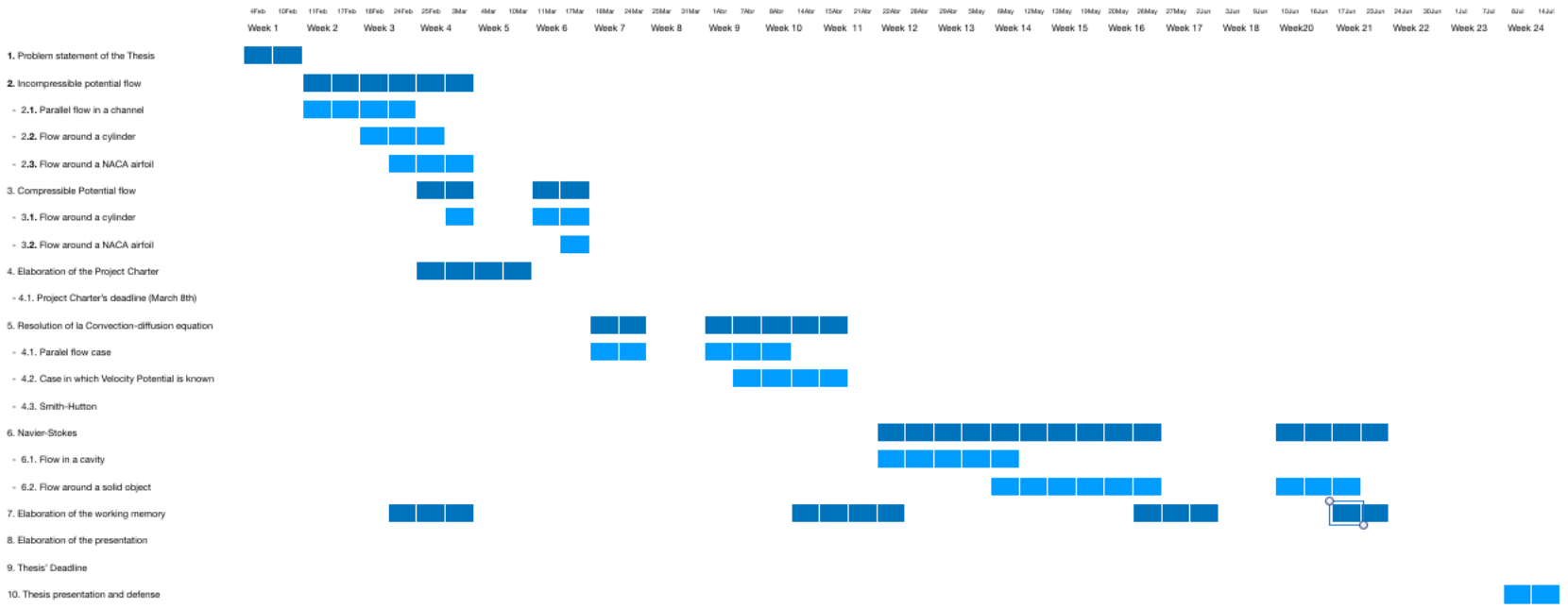

Figure 6.1: Diagram of Gantt

7 Conclusions and future activities

7.1 Conclusions

The main objective of the study was to learn and enlarge the knowledge about the physical phenomena that appears when a fluid interacts with a solid and with different external conditions. Throughout the study, the knowledge about fluid dynamics, heat transfer and programming skills have increased and improved.

In the elaboration of this study, there have been obtained solutions for different reference cases. These cases were selected wisely, most of them were academic cases for which there is an analytic solution or a computational solution has been obtained beforehand. Hence, the aim of solving these reference cases is to understand the governing principles and to expand this knowledge and abilities into more complex problems.

The first part consisted on a study of the potential flow equation in order to obtain the streamlines around different objects. Potential flow expression is obtained under the hypotheses of irrotational and inviscid, therefore potential flow can be a first and simple to obtain solution of a given problem.

Secondly, convection and diffusion terms were discussed deeply, the first term tends to order whereas the second tends to disorder and random behaviour. Also in this section, different numerical schemes were tried to solve the non-linearity of the convective term, numerical schemes were used to guess the value of a variable ϕ at the face. One important factor was the order of the scheme which depends on the number of grid points consulted to implement the approximation.

Finally, Driven Cavity problem was solved via Navier-Stokes (NS) equations. Previous sections were needed to comprehend the role of each term at NS equations. Fractional Step Method (FSM) was used in order to solve the computation of pressure and velocity field in each time step. Different Reynolds numbers (Re) were tested in the development of this section and it has been noted that reaching the steady state is more challenging when Re are high, a dense mesh is compulsory and computational time is tremendous.

To sum up, Computational Fluid Dynamics (CFD) is a combination of comprehending heat transfer and fluid dynamics principles, understanding the role of each term at Navier-Stokes equations, learning and applying mathematical theorems and principles to transform NS equations into numerical expressions and learning to develop a code for solving the problem and optimising it when possible.

7.2 Future activities

If the project could continue, there are different interesting lines to explore and to continue widen the knowledge about CFD:

- Compressible potential flow

  In this project, the potential flow solution obtained was incompressible. It would be interesting to test the solutions for compressible cases.

- Potential flow around a cylinder rotating

  Another interesting potential flow case would be to solve the potential flow around a cylinder rotating around its center. In the case solved in this study, the cylinder was static. Moreover, there is an analytic solution for this case so the possible solution obtained could be compared.

- Potential flow with wall method

  Potential flow that takes into account the boundary layer generated by the friction of the flow with surface.

- Different numerical schemes for convective terms

  Test different numerical schemes and homogenise the computational structure for any numerical scheme even if they are first, second or higher order.

- Optimise the code

  Make the code run faster and simplify calculus. It would be interesting to identify which calculus could be simplified as a matrix multiplied by a vector.

- Solve Differentiated Heated Driven Cavity

  Heated Driven Cavity has the same domain as the problem solved, however in this case temperature is involved, therefore a new term has to be taken into account (Conservation of Energy equation).

- Solve the flow around a cylinder and a square using NS equations and FSM to solve them

  Once developed the sequence of actions for the Driven Cavity case, next step will be to adapt the code for the case of a square or a cylinder in a duct. Boundary conditions will have to be changed, differentiate between body and fluid, use different meshes...

- Use unstructured meshes

  Implement the use of unstructured meshes using terms like connectivity matrix or even use triangular structured meshes.

8 Bibliography

References

[1] Jeremy Hanke & Deryl Snyder (STAR CCM+ Siemens) Prashanth Shankara. *Numerical Solution DLR-F11 High lift configuration using STAR-CCM+*. Tech. rep. 2014. URL: http://mdx2.plm.automation.siemens.com/presentation/numerical-simulation-dlr-f11-high-lift-configuration-using-star-ccm.

[2] F Moukalled, L Mangani, and M Darwish. *Fluid Mechanics and Its Applications The Finite Volume Method in Computational Fluid Dynamics*. Tech. rep. URL: http://www.springer.com/series/5980.

[3] CD Trias Miquel, FX ; Pérez-Segarra. *Analysis of Thermal and Fluid Issues - Introduction*. Tech. rep. Terrassa, Spain. URL: https://atenea.upc.edu/pluginfile.php/2754677/mod{_}resource/content/1/01{_}Introduction.pdf.

[4] Noel Black and Shirley Moore. "Gauss-Seidel Method". In: *MathWorld* (). URL: http://mathworld.wolfram.com/Gauss-SeidelMethod.html.

[5] A H Techet. *2.016 Hydrodynamics*. Tech. rep. URL: http://web.mit.edu/2.016/www/handouts/2005Reading4.pdf.

[6] Numerical Methods, Heat Transfer, and Fluid Dynamics. "Non-viscous flows". In: (), pp. 1–21.

[7] NASA. "Definition of Streamlines". In: *www.grc.nasa.gov* (). URL: http://www.grc.nasa.gov/WWW/k-12/airplane/stream.html.

[8] Nica D E Fluidos Prof and Aldo Tamburrino Tavantzis. "Flujo potencial bidimensional". In: (), pp. 1–12.

[9] National Aeronautics and Space Administration - NASA : Glenn Research Center. *Navier-Stokes Equations*. 2015. URL: https://www.grc.nasa.gov/www/k-12/airplane/nseqs.html (visited on 05/30/2019).

[10] Suhas V. Patankar. *Numerical heat transfer and fluid flow*. New York: Hemisphere Pub. Corp., 1980, p. 197. ISBN: 0891165223.

[11] Numerical Methods, Heat Transfer, and Fluid Dynamics. "Numerical resolution of the generic convection-diffusion equation". In: (), pp. 1–28.

[12] M S Darwish and F H Moukalled. *Normalized Variable and Space Formulation Methodology for High-Resolution Schemes*. Tech. rep. URL: https://www.aub.edu.lb/msfea/research/Documents/CFD-P58.pdf.

[13] Camilo Andrés Manrique. "Difusión-Convección: Problema Smith-Hutton". In: (2017). DOI: 10.13140/RG.2.2.31790.51523. URL: https://www.researchgate.net/publication/317813607.

[14] CTTC-UPC. *A3-A Two-dimensional Steady Convection-Diffusion Equation: the Smith-Hutton problem*. Tech. rep. URL: https://atenea.upc.edu/pluginfile.php/2714332/mod{_}resource/content/3/A3{_}Exercise-Smith-Hutton.pdf.

[15] The Visual Room. *1. Poisson Equation for Pressure*. URL: http://www.thevisualroom.com/poisson{_}for{_}pressure.html (visited on 05/25/2019).

[16] Frederic N Felten and Thomas S Lund. *Critical Comparison of the Collocated and Staggered Grid Arrangements for Incompressible Turbulent Flows*. Tech. rep. URL: https://pdfs.semanticscholar.org/9c8f/938a29bdc8b5a82c32192b3634b5aebf0pdf.

[17] C. M. Rhie and W. L. Chow. "Numerical study of the turbulent flow past an airfoil with trailing edge separation". In: *AIAA Journal* 21.11 (1983), pp. 1525–1532. ISSN: 0001-1452. DOI: 10.2514/3.8284. URL: http://arc.aiaa.org/doi/10.2514/3.8284.

[18] *CMEE | EM Lab*. URL: http://emlab.utep.edu/ee4386{_}5301{_}CompMethEE.htm (visited on 05/25/2019).

[19] CFD Wiki. *Odd-even decoupling of cells - CFD*. URL: https://www.cfd-online.com/Forums/main/3548-odd-even-decoupling-cells.html (visited on 05/28/2019).

[20] CFD Wiki. *Staggered grid – CFD-Wiki*. URL: https://www.cfd-online.com/Wiki/Staggered{_}grid (visited on 05/28/2019).

[21] Robert W. Fox, Alan T. McDonald, and Philip J. Pritchard. *Introduction to fluid mechanics*. 6th. Hoboken: Wiley, 2004, p. 787. ISBN: 9780471202318.

[22] U Ghia, K.N Ghia, and C.T Shin. "High-Re solutions for incompressible flow using the Navier-Stokes equations and a multigrid method". In: *Journal of Computational Physics* 48.3 (1982), pp. 387–411. ISSN: 00219991. DOI: 10.1016/0021-9991(82)90058-4. URL: https://linkinghub.elsevier.com/retrieve/pii/0021999182900584.

[23] *MacBook Air (11 inch, mid 2011) - Specs*. URL: https://support.apple.com/kb/sp631?locale=es{_}ES (visited on 06/01/2019).

[24] *Red Eléctrica de España | Series estadísticas nacionales*. URL: https://www.ree.es/es/estadisticas-del-sistema-electrico-espanol/series-estadisticas/series-estadisticas-nacionales (visited on 06/01/2019).